



Cite this: *Biomater. Sci.*, 2022, **10**, 2462

## Articulation inspired by nature: a review of biomimetic and biologically active 3D printed scaffolds for cartilage tissue engineering

Donagh G. O'Shea, <sup>a,c</sup> Caroline M. Curtin <sup>a,b,c</sup> and Fergal J. O'Brien <sup>\*a,b,c</sup>

In the human body, articular cartilage facilitates the frictionless movement of synovial joints. However, due to its avascular and aneural nature, it has a limited ability to self-repair when damaged due to injury or wear and tear over time. Current surgical treatment options for cartilage defects often lead to the formation of fibrous, non-durable tissue and thus a new solution is required. Nature is the best innovator and so recent advances in the field of tissue engineering have aimed to recreate the microenvironment of native articular cartilage using biomaterial scaffolds. However, the inability to mirror the complexity of native tissue has hindered the clinical translation of many products thus far. Fortunately, the advent of 3D printing has provided a potential solution. 3D printed scaffolds, fabricated using biomimetic biomaterials, can be designed to mimic the complex zonal architecture and composition of articular cartilage. The bioinks used to fabricate these scaffolds can also be further functionalised with cells and/or bioactive factors or gene therapeutics to mirror the cellular composition of the native tissue. Thus, this review investigates how the architecture and composition of native articular cartilage is inspiring the design of biomimetic bioinks for 3D printing of scaffolds for cartilage repair. Subsequently, we discuss how these 3D printed scaffolds can be further functionalised with cells and bioactive factors, as well as looking at future prospects in this field.

Received 30th September 2021,  
Accepted 17th March 2022

DOI: [10.1039/d1bm01540k](https://doi.org/10.1039/d1bm01540k)

[rsc.li/biomaterials-science](http://rsc.li/biomaterials-science)

## 1. Introduction

“Innovation inspired by nature” – this is how biomimicry is described by author and scientist Janine M. Benyus in her 1997 book of the same title and although a relatively new term, the concept of biomimicry is evident throughout the history of human innovation.<sup>1,2</sup> From the study of birds to inspire the design of aeroplanes to the study of human anatomy to inspire next generation medical devices, mimicking nature has allowed us to create innovative new technologies and improve our own quality of life.

But how does biomimicry apply to tissue engineering (TE)? TE, also known as regenerative medicine, is an emerging multi-disciplinary field of modern medicine which uses a combination of biomaterials, cells and bioactive factors or gene therapeutics, sometimes referred to as the ‘TE triad’, to bioengineer living tissues for a range of applications.<sup>3</sup> These diverse applications range from disease modelling<sup>4</sup> and organ-on-a-chip develop-

ment,<sup>5</sup> to the regeneration of a variety of tissue types including cardiac tissue,<sup>6</sup> musculoskeletal tissue<sup>7</sup> and skin,<sup>8</sup> amongst others. In essence, the field of TE relies on the fabrication of biomaterial implants called ‘scaffolds’, which can support cell growth and whose microenvironment, architecture and functionality mimic that of native human tissue. Therefore, it could be argued that biomimicry forms the foundations of the field of TE.

In recent years, TE scaffolds have grown in popularity as a potential treatment option for a range of conditions. In the field of orthopaedic medicine, for example, these scaffolds have emerged as a promising treatment option for chondral defects (CDs), which are localised areas of damage to the articular cartilage of a synovial joint. In severe cases, the defect can penetrate into the underlying subchondral bone leading to the formation of an osteochondral defect.<sup>9</sup> Once the friction-reducing articular cartilage tissue has worn away, the underlying bone surfaces can rub against one another causing significant stiffness and pain, thus hindering joint mobility.<sup>10</sup> CDs can be caused by traumatic injury or wear and tear over time and can lead to the development of osteoarthritis, a degenerative joint disease which affects 9.6% of men and 18% of women over the age of 60 years worldwide.<sup>11</sup> Unfortunately, due to the avascular and aneural nature of articular cartilage, these defects will not heal on their own.

Current treatment options for CDs include surgical procedures such as microfracture, autograft or allograft pro-

<sup>a</sup>Tissue Engineering Research Group, Department of Anatomy and Regenerative Medicine, RCSI University of Medicine and Health Sciences, Dublin, Ireland.  
E-mail: [fjobrien@rcsi.ie](mailto:fjobrien@rcsi.ie)

<sup>b</sup>Trinity Centre for Biomedical Engineering, Trinity College Dublin, Ireland  
<sup>c</sup>Advanced Materials and Bioengineering Research Centre (AMBER), RCSI and TCD, Dublin, Ireland



cedures, or cell-based techniques.<sup>12</sup> Microfracture is a procedure whereby tiny fractures are made in the subchondral bone allowing the release of bone marrow stem cells into the defect which ultimately develop into fibrocartilage.<sup>13</sup> However unlike articular cartilage, fibrocartilage is rich in collagen type I and thus possesses inferior mechanical properties. Autograft procedures, such as osteochondral autograft transfer systems (OATS) and mosaicplasty, involve transplanting osteochondral tissue from low load bearing regions of the knee into defects located in high load bearing regions.<sup>14,15</sup> However the procedure is only suitable for smaller defects due to limited tissue availability at the donor site and can also be associated with donor site morbidity due to infection. Allografts are articular cartilage transplants taken from another donor and thus are not constrained by tissue availability at the donor site. However the availability of donors and the risk of the patient's immune system rejecting the graft limits the use of this procedure.<sup>16,17</sup> Cell-based procedures such as autologous chondrocyte implantation (ACI) have shown promise and involve removing cells from healthy articular cartilage, expanding them in culture and then implanting the expanded chondrocytes into the chondral defect under a collagen membrane. However dedifferentiation of the chondrocytes during *in vitro* cell expansion can occur leading to a reduced capacity of the cells to lay down new ECM when implanted back into the defect.<sup>18</sup> Therefore, despite providing much needed symptomatic relief to patients, current surgical procedures are not without limitations, often resulting in a variable healing response and the formation of non-durable tissue.<sup>16,19</sup> This issue becomes even more prominent following surgical treatment of larger defects.<sup>20</sup>

Without successful intervention, the osteoarthritic joint can deteriorate to a point where total joint replacement is the only remaining option to relieve pain and discomfort. Total joint replacement involves complete removal of the arthritic joint and insertion of a prosthesis in its place. These prostheses are typically made from a metal such as a titanium alloy, polymers, ceramics or a composite.<sup>21</sup> Although total joint replacement can result in dramatic improvements in patient quality of life following initial post-operative rehabilitation, revision surgery can be required over time due to implant failure. While the lifetime risk of requiring revision surgery is relatively low in patients aged over 70 years (1–6%), this risk is significantly higher in younger patients with 1 in 3 patients aged 50 to 55 years likely to require revision surgery. More than half of these revision surgeries are needed within 6 years of the initial joint replacement surgery.<sup>22</sup> Therefore the benefits of this procedure need to be weighed against the potential risk of future surgeries and poor health outcomes, particularly for younger patients.

Several fabrication techniques have been investigated to engineer scaffolds which could be surgically implanted into these defects in order to support regrowth of cartilage and/or bone tissue. Examples of these techniques including electrospinning,<sup>23–29</sup> solvent casting/melt moulding and particulate leaching,<sup>30–33</sup> freeze drying<sup>34–36</sup> and gas foaming

techniques,<sup>37–42</sup> amongst others. Scaffolds for bone and cartilage repair fabricated using the freeze drying method have been the subject of extensive research here in the RCSI Tissue Engineering Research Group (TERG). Using a controlled freeze drying cycle, our lab fabricates highly porous scaffolds from slurries of biomaterials native to the human body such as collagen type I, hyaluronic acid (HyA) and chondroitin sulfate (CS).<sup>43–47</sup> The composition and stiffness of these scaffolds can be tailored to promote cartilage or bone regeneration as required.<sup>44</sup>

While significant progress in the field of TE for cartilage repair has been made using scaffolds fabricated *via* the techniques outlined above, the inability to mimic the complexity of native tissue has hindered the clinical translation of many products thus far.<sup>48,49</sup> Fortunately, the development of 3D printed scaffolds has provided a potential solution. These scaffolds can be designed to mirror the complex zonal architecture of articular cartilage and can be reinforced with polymers to improve their mechanical strength. The biomaterial inks used to print these scaffolds can also be functionalised with cells such as mesenchymal stem cells (MSCs) or mature chondrocytes, bioactive factors such as growth factors, or gene therapeutics such as plasmid DNA (pDNA) or microRNA (miR) to promote cartilage growth.<sup>50–53</sup> These functionalised biomaterial inks are also called 'bioinks'.<sup>54</sup> There are a number of 3D printing techniques used in this field including droplet-based,<sup>54–56</sup> laser-based<sup>57,58</sup> and extrusion-based methods.<sup>5</sup> However, due to its versatility and compatibility with cells and a wide range of biomaterials, extrusion-based 3D printing is one of the most popular 3D printing methods in the field of TE for cartilage repair.<sup>59,60</sup> Thus, this review will focus on the development of bioinks for extrusion-based 3D printing only.

In the field of 3D printing for cartilage repair, there is an ever growing emphasis placed on the importance of designing advanced biomimetic bioinks whose matrix composition reflects that of native articular cartilage. This biomimetic approach helps in the regeneration of functional tissue and minimises adverse reactions when the 3D printed scaffold is implanted *in vivo*. Therefore, the scope of this review will focus on how the architecture and composition of native articular cartilage is inspiring the design of biomimetic bioinks for extrusion-based 3D printing of scaffolds for cartilage repair.

## 2. Architecture and composition of articular cartilage

Articular cartilage performs two crucial functions in human synovial joints – the first is to facilitate frictionless movement of the joint, and the second is to withstand repeated compressive loading. Both the architecture and the composition of the tissue play a significant role in facilitating these functions. Therefore, a thorough understanding of the structure and both the biomaterial and cellular composition of native articular cartilage is crucial when designing biomimetic bioinks for cartilage repair.



## 2.1. Architecture of articular cartilage

The extracellular matrix (ECM) of articular cartilage is largely composed of collagen (primarily type II), proteoglycans and water.<sup>61</sup> This ECM is synthesised and maintained by highly specialised cells known as chondrocytes whose morphology, density and organisation varies with cartilage depth leading to the formation of three distinct zones within the articular cartilage.<sup>62</sup> The uppermost superficial zone (10–20% articular cartilage thickness) is characterised by the presence of high density flattened chondrocytes embedded in an ECM with collagen fibres aligned parallel to the joint surface and the presence of the lubricant proteoglycan 4 (PRG4 or lubricin). The middle zone (40–60% articular cartilage thickness) consists of rounded chondrocytes within a more disorganised collagen matrix, while the deep zone (30–40% articular cartilage thickness) consists of large chondrocytes surrounded by a pericellular matrix consisting of collagen type VI, and thicker collagen fibres organised perpendicular to the joint surface.<sup>63,64</sup> The deep zone is then underpinned by calcified cartilage and the subchondral bone. The structure of articular cartilage is outlined in Fig. 1 below.

## 2.2. Composition of articular cartilage

Collagen is a protein consisting of a triple helix of three polypeptide chains called  $\alpha$ -chains, and is the primary macromolecule component found in the ECM of articular cartilage.<sup>65</sup> There are many different types of collagen present in the human body however fibril-forming collagens, such as collagen types I and II, are by far the most abundant.<sup>66</sup> Collagen type I, which is the main collagen type found in fibrocartilage,

consists of two  $\alpha 1(I)$  chains and one  $\alpha 2(I)$  chain. In contrast, collagen type II, which is the primary collagen type found in articular cartilage, consists of three identical  $\alpha 1(II)$  chains which contain a higher proportion of hydroxylysine, glucosyl and galactosyl residues. These residues mediate interactions with surrounding proteoglycans in the ECM of articular cartilage.<sup>65</sup> The tightly packed collagen type II and IX fibres found aligned parallel to the articulating surface in the superficial zone of articular cartilage are also largely responsible for its tensile properties.<sup>64</sup>

Proteoglycans are the second largest macromolecule component of articular cartilage and consist of a protein core with glycosaminoglycan (GAG) side chains. GAGs are negatively charged polysaccharides and can be non-sulfated, such as HyA, or sulfated, such as CS or keratin sulfate. Aggrecan is the most abundant proteoglycan found in articular cartilage and interacts with HyA to form large negatively charged aggregates within the matrix of collagen type II fibrils.<sup>67</sup> Water comprises 60–80% of the wet weight of cartilage and in this aqueous environment, aggrecan molecules become hydrated and swell. This swelling is resisted by the surrounding collagen fibrils, leading to the formation of an equilibrium between the swelling forces of aggrecan and the tensile forces of the collagen matrix.<sup>68,69</sup> This is the mechanism by which articular cartilage withstands repeated compressive loading so effectively.

## 2.3. Chondrocytes – the resident cells of articular cartilage

As mentioned above, chondrocytes are the primary cell type found in articular cartilage and play an integral role in the synthesis and maintenance of articular cartilage ECM. In the

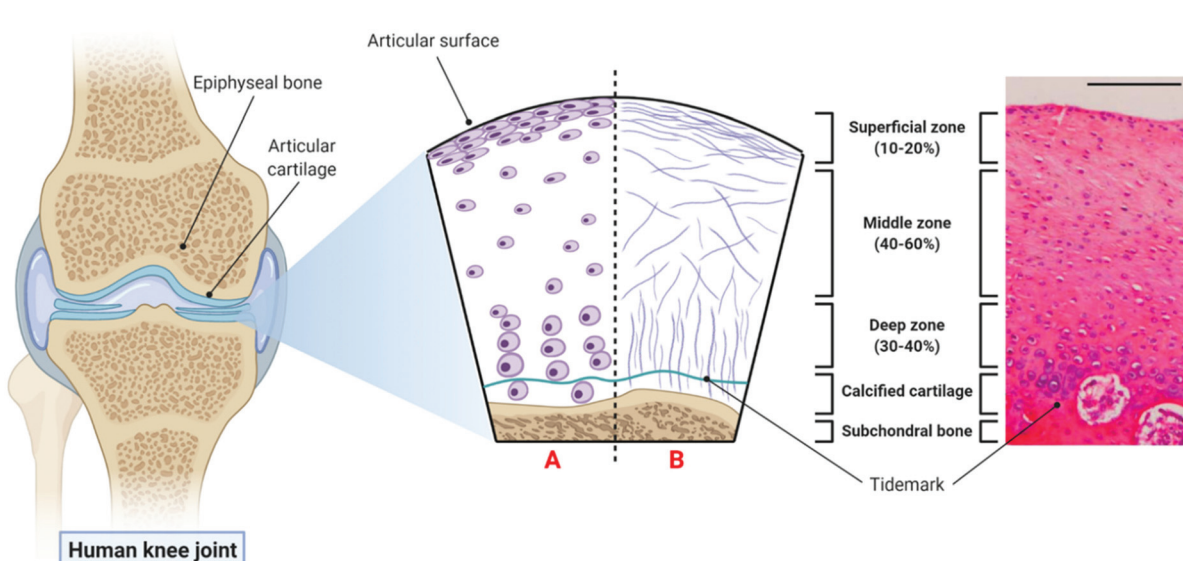


**Fig. 1** The structure of articular cartilage – the diagram on the left shows a synovial joint with a cross-sectional schematic depicting healthy articular cartilage: A – morphology and organisation of chondrocytes in the superficial, middle and deep zones respectively; B – orientation of collagen fibres in the superficial, middle and deep zones respectively. The histological image (haematoxylin and eosin (H&E) staining) on the right is taken from the femoral condyle of a rabbit knee joint and demonstrates the zonal distribution of chondrocytes within articular cartilage (scale bar = 100  $\mu$ m). Histological image reproduced and adapted from Matsiko *et al.*<sup>62</sup> with permission from MDPI (Copyright © 2013, MDPI). Figure created with Biorender.com.



superficial and middle zones, chondrocytes primarily synthesise collagen types II, IX and XI and aggrecan, all of which are critical to the compressive and tensile properties of the tissue. However, in the deep zone, terminally differentiated chondrocytes mainly produce collagen type X and aggrecan.<sup>70</sup> However, despite the importance of these cells, chondrocytes make up just 2% of the total cartilage tissue volume in a healthy adult and so are present in quite a small quantity.<sup>71</sup> This sparse distribution means that very little cell-cell contact occurs within the tissue, therefore chondrocyte activity is largely dictated by interactions with the surrounding ECM.<sup>72</sup>

During development, chondrocytes are formed following exposure of mesenchymal stem cells (MSCs) to certain biological cues in a process known as chondrogenesis. MSCs are a type of stem cell which are capable of differentiating into several connective tissue cell types including those from an adipogenic, osteogenic and chondrogenic lineage, depending on exposure to defined conditions.<sup>73,74</sup> Chondrogenesis begins with proliferation and condensation of MSCs, leading to the initiation of cell-ECM and cell-cell interactions *via* gap junctions, and ultimately the formation of chondroprogenitor cells.<sup>75</sup> Following this, chondroprogenitor cells differentiate into chondrocytes and this stage is characterised by the deposition of the cartilage ECM components collagen types II, IX and XI, and aggrecan.<sup>76</sup> Production of these ECM components is a direct result of the expression of the genes Col2a1, Col9A1, Col11a1 and ACAN, and thus these genes are often considered to be markers of chondrogenesis in the field of TE for cartilage

repair. This process is driven by a number of growth factors including bone morphogenetic proteins (BMPs), transforming growth factor- $\beta$ 1 and 3 (TGF- $\beta$ 1 and 3) and insulin-like growth factor-1 (IGF-1).<sup>77</sup> The transcription factors, SOX-5, 6 and 9 (known as the SOX-trio), also play a key role in promoting chondrogenesis with SOX-9, in particular, directly influencing up-regulation of pro-chondrogenic genes such as Col2a1 and ACAN.<sup>78</sup>

In the formation of articular cartilage, the chondrogenic pathway stops here. However, chondrocytes can undergo terminal differentiation to form hypertrophic chondrocytes, which eventually leads to ossification of the tissue.<sup>79</sup> This process is known as endochondral ossification and is the way in which long bones are formed during foetal development. These hypertrophic chondrocytes synthesise collagen type X (regulated by the gene Col10a1), and also express the enzymes matrix metalloproteinase-13 (MMP-13) and alkaline phosphatase (ALP), which are involved in the degradation of cartilage ECM and regulation of bone mineralisation respectively.<sup>76,80,81</sup> Thus, the expression of Col10a1, MMP-13 and ALP are often considered markers of hypertrophy in cartilage TE.<sup>82</sup> The transcription factor Runx2 is also known to promote chondrocyte hypertrophy, and the growth factor, vascular endothelial growth factor (VEGF), plays a key role in vascularisation of the tissue during endochondral ossification.<sup>83,84</sup> In healthy articular cartilage, hypertrophic chondrocytes are found in the deep zone, near the border with the subchondral bone.<sup>64</sup> The chondrogenic pathway is outlined in Fig. 2 below.

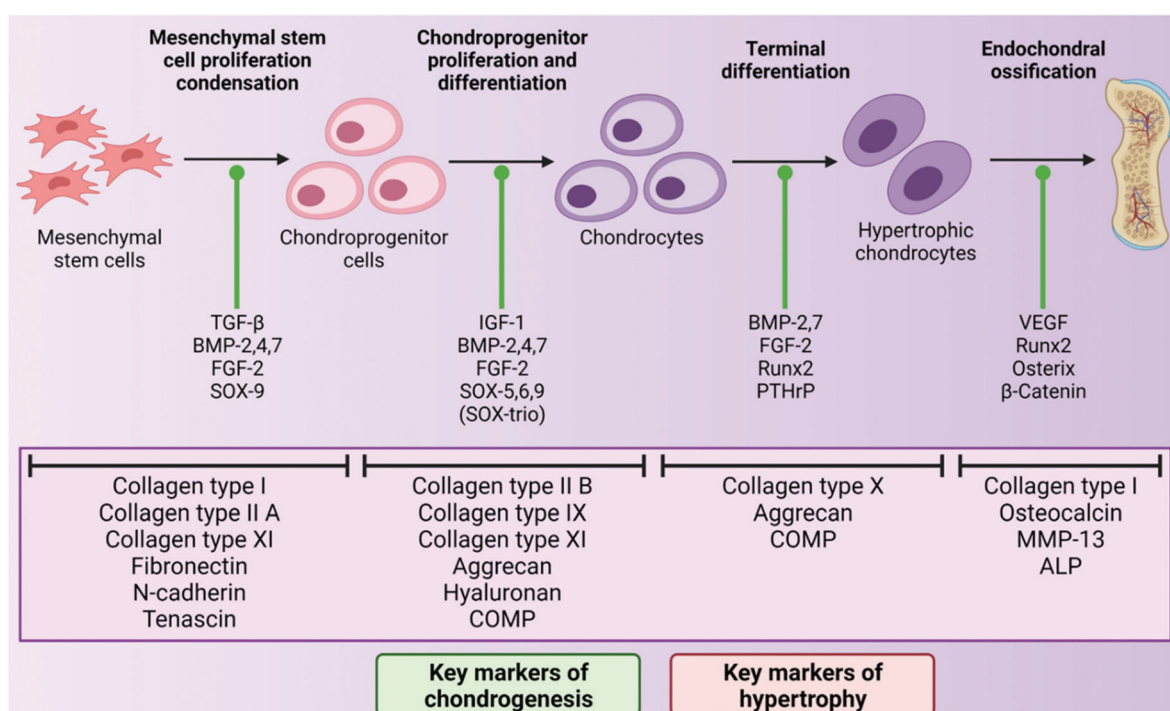


**Fig. 2** A schematic of the process of chondrogenesis, starting with MSC proliferation and condensation and ending with endochondral ossification. The factors that promote transition from one stage of the chondrogenic pathway to the next are highlighted with a green indicator. The characteristic ECM proteins of each stage are highlighted below. Figure created with Biorender.com.



### 3. Biomimetic 3D printed scaffolds for cartilage repair

When designing a biomimetic 3D printed scaffold for cartilage repair, there are several key considerations which should be taken into account based on the biomaterial and cellular composition of native articular cartilage. Firstly, a highly hydrated environment is crucial not only to cell survival, but also to the biofunctionality of the tissue. From a 3D printing perspective, hydrogels are well placed to provide such an environment. Hydrogels are hydrophilic polymer networks which are extensively water swollen and are already widely employed as bioink components throughout the field of TE.<sup>85</sup> Secondly, several biomaterials such as collagen, HyA and CS play a synergistic role in the unique mechanical and biological functions of articular cartilage and thus are desirable as bioink components. Thirdly, chondrocytes are required for tissue regeneration and thus the bioink could be functionalised with MSCs, chondroprogenitor cells or mature chondrocytes to accelerate healing. However, these cells must also be provided with appropriate biological cues in order for them to differentiate into, or maintain, a chondrogenic lineage and prevent hypertrophy.

The physiochemical and rheological properties of the bioink used to develop the scaffold are also a key consider-

ation. An ideal bioink should exhibit a decrease in viscosity during the printing process to allow extrusion (*i.e.* possess shear thinning properties), but also be capable of crosslinking immediately post-printing to retain its shape and ensure mechanical stability of the 3D printed construct.<sup>86,87</sup> In addition to this, the 3D printed scaffold must also be sufficiently porous to facilitate the attachment, proliferation and differentiation of cells, as well as allowing diffusion of solutes and nutrients and deposition of ECM.<sup>54,88</sup> This is often influenced by the polymer concentration or the crosslink density of the bioink. The bioink, and thus the 3D printed scaffold, must also be biodegradable at a rate appropriate to that of the regenerating tissue to allow for gradual replacement of the scaffold with deposited ECM from native cells.<sup>89</sup> It is also critical that both the bioink and its degradation products are non-toxic and non-immunogenic.<sup>3</sup> The ideal properties of a bioink are summarised in Fig. 3 below.

#### 3.1. Mimicking the composition of articular cartilage when developing 3D printed scaffolds

Strategies for fabricating biomimetic 3D printed scaffolds for cartilage repair strive to maintain the synergistic biofunctionality of native biomaterials by using biomimetic bioink formulations with desirable physiochemical and rheological pro-

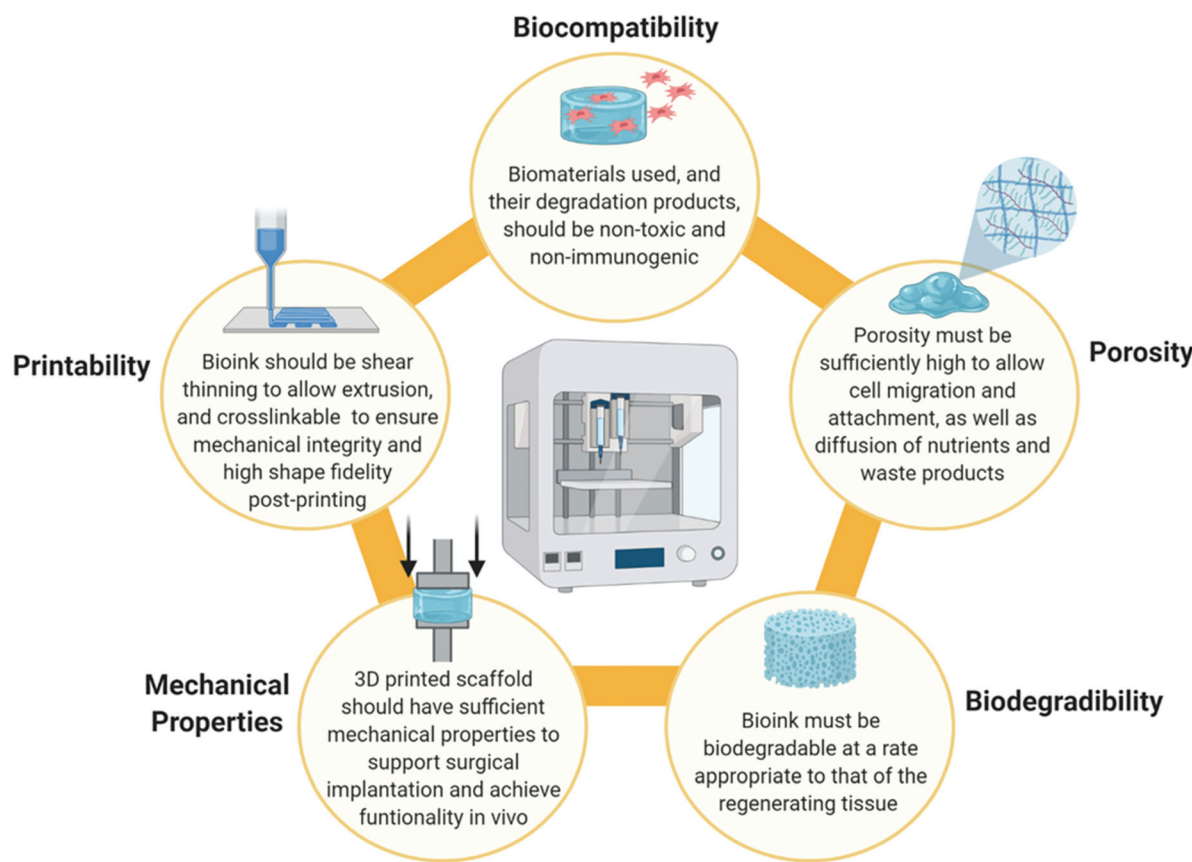


**Fig. 3** A summary of the ideal bioink properties to facilitate 3D printing of biomaterial scaffolds with high shape fidelity and to promote regeneration of cartilage tissue when the scaffold is implanted *in vivo*. Figure created with Biorender.com.



perties. This can be challenging as many biomaterials native to human articular cartilage do not innately possess good 3D printing properties. The following sections will look at how native biomaterials are being adapted to formulate biomimetic bioinks for cartilage repair with favourable 3D printing properties.

**3.1.1. Collagen bioinks for cartilage repair.** The incorporation of collagen into bioinks for cartilage repair is an obvious target due to its innate biocompatibility and the role it plays within the ECM of native articular cartilage. Collagen also possesses naturally occurring cell binding sites in the form of the amino acid motif Arg-Gly-Asp (RGD), and so can easily facilitate cell adhesion and growth.<sup>90</sup> The vast majority of collagen containing bioinks for cartilage repair reported in the literature are formulated using the fibril-forming collagen type I (COL-I). However, despite the advantages of incorporating collagen into bioinks for cartilage repair, it is a notoriously challenging biomaterial to work with. COL-I exists as a liquid at lower temperatures and low pH but as the temperature and pH tend towards physiological conditions (37 °C and pH 7.4), COL-I molecules start to self-assemble into fibrils leading to hydrogel formation.<sup>91</sup> These collagen hydrogels, however, tend to be mechanically weak and the fibrillation process is difficult to control and can take up to 30 minutes at 37 °C which is problematic for shape retention and mechanical stability post-printing.<sup>92</sup> Several strategies have been employed to overcome these challenges whilst still maintaining the natural biofunctionality of COL-I.

One such approach involves controlling the physical cross-linking of COL-I hydrogels *via* the manipulation of hydrogel concentration, pH and temperature. Traditionally, COL-I hydrogels were formulated at lower concentrations of <10 mg mL<sup>-1</sup> in acetic acid; however, these hydrogels were not cell friendly and they possessed very poor mechanical properties.<sup>93</sup> However, more recent studies have been successful in formulating high concentration (up to 20 mg mL<sup>-1</sup>), neutralised COL-I hydrogels by carefully adjusting and buffering the pH of the formulation to physiological pH and salt concentration.<sup>94</sup> Very high concentration COL-I hydrogels are also now available as commercial bioink formulations such as Lifeink® 200 (Advanced BioMatrix, CA, USA) which contains 35 mg mL<sup>-1</sup> COL-I, or Viscoll (Imtek Ltd, Russia) which contains up to 80 mg mL<sup>-1</sup> COL-I.<sup>95,96</sup> These high concentration COL-I bioinks possess better 3D printing properties and mechanical properties than lower concentration COL-I formulations, resulting in greater shape fidelity of the printed construct and they can also support 3D bioprinting of cells.<sup>97,98</sup> However, temperature control when 3D printing with COL-I bioinks is critical – the print head should be maintained at 4–10 °C to facilitate printing of the bioink, but the print bed should be maintained at 37 °C to facilitate thermal crosslinking of the deposited bioink filaments.<sup>94,99</sup> COL-I prints can also be further crosslinked post-printing using cell friendly chemical crosslinkers such as genipin.<sup>100,101</sup>

Another approach to improving the mechanical properties of COL-I bioinks involves chemically modifying the COL-I

hydrogel with crosslinkable chemical groups. The COL-I molecule may be chemically modified at the primary amine site on the lysine residue with photocrosslinkable methacrylate groups to form methacrylated collagen (ColMA).<sup>102–105</sup> This allows the COL-I bioink to be crosslinked in the presence of a photoinitiator, such as Irgacure 2959 (I2959) or lithium phenyl-2,4,6-trimethylbenzoylphosphinate (LAP), and UV light during or immediately following the printing process. The addition of methacrylate groups has also been shown to confer thermoreversible gelation properties to the hydrogel without affecting the fibrillation process, biodegradability or bioactivity of COL-I.<sup>103,106</sup> Similarly, COL-I has also been functionalised with norbornene groups to form a thiol-ene photocrosslinkable hydrogel which was shown to have improved 3D printing properties without a loss of bioactivity.<sup>107</sup>

Sacrificial support baths, as employed in Freeform Reversible Embedding of Suspended Hydrogels (FRESH), can also be used to facilitate 3D printing of COL-I bioinks.<sup>108</sup> The FRESH method of 3D printing involves 3D printing a bioink into a thermoreversible gelatin slurry support bath which exhibits yield-stress rheological behaviour, similar to that exhibited by Bingham plastic fluids. This rheological phenomenon facilitates seamless movement of the print needle through the support bath while extruding the bioink, while also embedding the printed filament into the support bath to maintain the shape fidelity of the 3D printed construct<sup>109</sup> (Fig. 4). The support bath can also be supplemented with specific cross-linking agents to crosslink the construct as it prints and once the print is completed, the support bath can be melted away at 37 °C. When 3D printing with a COL-I based bioink, the FRESH support bath is supplemented with a neutral pH buffer such as phosphate buffered saline (PBS) or 4-(2-hydroxyethyl) piperazine-1-ethanesulfonic acid (HEPES) buffer to allow fibrillation to occur. The fibrillation process is then completed upon incubation of the prints at 37 °C for at least 30 minutes and the melted gelatin slurry can then be discarded. This method has been used to 3D print complex biological structures using both low concentration,<sup>108</sup> and high concentration<sup>110,111</sup> COL-I bioink formulations.

Collagen can also be partially hydrolysed to form gelatin, which is often used to formulate bioinks for cartilage repair. Gelatin has superior solubility and rheological properties when compared to native collagen and it also retains the RGD cell binding motif which is present in native collagen.<sup>112</sup> Thus, it is a popular biomimetic collagen substitute for 3D printing purposes. Gelatin is also biocompatible and biodegradable, and already has approval from the United States Food and Drug Administration (US FDA) for use in the food and biomedical industry, thus it does not present the same regulatory hurdles as other biomaterials.<sup>113</sup> However, gelatin in its unmodified state is not suitable for TE applications due to its low viscosity at body temperature.<sup>114</sup> Therefore, gelatin is often incorporated into composite bioink formulations with other biomaterials such as silk fibroin<sup>115–117</sup> or alginate,<sup>118</sup> or else chemically modified to confer crosslinking functionality to the molecule. The most common example of this is the chemical



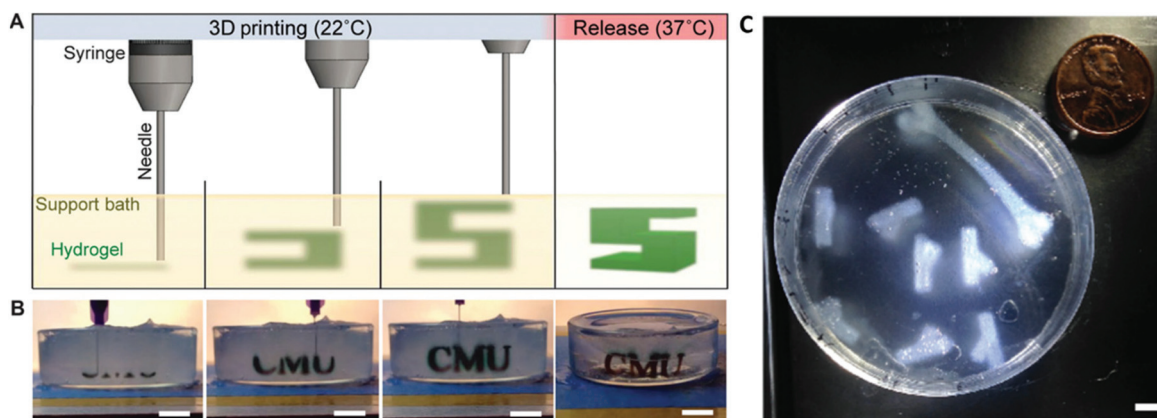


**Fig. 4** FRESH 3D printing is conducted by extruding a bioink into a thermoreversible gelatin slurry support bath which can subsequently be melted and removed by heating to 37 °C (A and B). Heating to 37 °C also allows thermal fibrillation of collagen-based bioinks to occur. The FRESH gelatin slurry provides mechanical support to the 3D printed bioink filaments and facilitates 3D printing of complex anatomical structures using collagen-based bioinks (C). A, B and C are re-printed and adapted with from Hinton *et al.*<sup>108</sup> with permission from the American Association for the Advancement of Science (AAAS) (Copyright © 2015, The Authors).

modification of gelatin with methacrylate groups to form gelatin methacrylate (GelMA).<sup>119,120</sup> Similar to ColMA, GelMA is photocrosslinkable in the presence of a photoinitiator, such as I2959 or LAP, and UV light, and both GelMA-only bioinks and GelMA-containing composite bioinks have been shown to be biocompatible and promote regeneration of cartilage tissue.<sup>121–126</sup> Lim *et al.* also further built on the functionality of GelMA by chemically modifying the molecule with tyrosine residues which aid integration of the 3D printed scaffold into the chondral defect.<sup>127</sup>

**3.1.2. Hyaluronic acid bioinks for cartilage repair.** Hyaluronic acid (HyA) is a non-sulfated GAG consisting of repeating disaccharide units of D-glucuronic acid and N-acetyl-D-glucosamine which is ubiquitous within the human body.<sup>128</sup> In articular cartilage, HyA plays a crucial role in the load-bearing and friction-reducing properties of the tissue, and so it is a desirable biomaterial in the field of TE for cartilage repair.<sup>128,129</sup> HyA also interacts with MSCs and chondrocytes *via* CD44 cell surface receptors, which serve to anchor cells to proteoglycan aggregates in articular cartilage *in vivo*, and also contribute to the synthesis and maintenance of cartilage ECM.<sup>130</sup> The critical role that HyA plays in promoting cartilage regeneration has been repeatedly highlighted in the literature, where HyA and its derivatives have been shown to possess innate chondrogenic properties.<sup>131–140</sup>

Due to their innate biocompatibility, chondrogenic potential and shear thinning properties, HyA hydrogels are popular as bioink formulations for cartilage repair.<sup>141</sup> However, the main drawback with these hydrogels is that they are not readily crosslinkable for 3D printing applications and so have poor shape retention post-printing.<sup>142</sup> Therefore, when used to formulate bioinks, HyA hydrogels are often blended with other biomaterials or chemically modified to confer crosslinking functionality to the bioink. Biomaterials commonly blended with HyA to formulate bioinks for cartilage repair include

hydrogels such as alginate, which crosslinks in the presence of divalent cations,<sup>143–146</sup> or GelMA,<sup>147</sup> which is photocrosslinkable, amongst others. As alginate is also a hydrophilic linear polysaccharide, it is sometimes employed as a crosslinkable GAG mimetic, and may even be sulfated to further mimic naturally occurring sulfated GAGs such as CS.<sup>148</sup> However, as alginate hydrogels do not possess any naturally occurring cell-binding moieties,<sup>149</sup> blending with HyA can facilitate improved cell adhesion to the bioink.

HyA is also quite a chemically versatile molecule and can be modified at the carboxyl, hydroxyl and amide groups respectively to confer a wide range of crosslinking functionality.<sup>150</sup> Similar to ColMA and GelMA which are discussed above, HyA can also be chemically modified with photocrosslinkable methacrylate groups to form methacrylated HyA or HyA methacrylate (often abbreviated to 'MeHA' or 'HAMA') which crosslinks in the presence of UV light and a photoinitiator.<sup>123,151–156</sup> Modification of HyA with other chemical groups such as norbornene groups,<sup>157</sup> thiols,<sup>158,159</sup> and amino acid derivatives,<sup>160,161</sup> amongst others, also allow for the formation of crosslinkable hydrogels. Furthermore, the HyA molecule can be modified to allow for protein-ligand binding (*e.g.* biotin-avidin binding system) or enzymatic crosslinking functionality which has been shown to improve the printability of the hydrogels, and promote subsequent cell adhesion and proliferation.<sup>162,163</sup> Some studies also report blending modified HyA and other biomaterials, such as alginate, to further improve the 3D printing properties and chondrogenic potential of the bioink,<sup>162</sup> or co-printing with thermoplastics such as PLA or PCL to improve the mechanical properties of the 3D printed scaffold.<sup>143,158,159</sup>

However, when chemically modifying HyA hydrogels, it is important to consider the effects of the modification on the physiochemical properties and overall biofunctionality of the HyA molecule. For example, the carboxylic acid group on the

glucuronic acid subunit is deprotonated at physiological pH and thus confers a negative charge on the molecule *in vivo*.<sup>164</sup> This negative charge largely contributes to the swelling properties of HyA as the HyA hydrogel becomes hydrated and swells in response to electrostatic repulsion between adjacent deprotonated carboxylic acid groups.<sup>165</sup> Therefore, chemical modification of the HyA molecule at the carboxylic acid group can affect the overall charge of the molecule and thus the swelling properties of the hydrogel. Similarly, chemical modification of HyA can also affect cell interactions with the hydrogel *via* CD44 binding. Kwon *et al.* demonstrated that high degrees of HyA chemical modification (approximately 40%) can negatively affect CD44-hydrogel interactions and subsequently have negative effects on MSC chondrogenesis in cell-laden hydrogels. However, HyA hydrogels with a lower degree of modification (approximately 10–20%) still exhibit improved CD44 binding and chondrogenic potential when compared to inert hydrogels.<sup>154</sup> Therefore, the degree of HyA modification is an important consideration when formulating biomimetic bioinks for cartilage repair using modified HyA hydrogels.

**3.1.3. Chondroitin sulfate bioinks for cartilage repair.** Chondroitin sulfate (CS) is a sulfated GAG and, as previously mentioned, is mostly present in articular cartilage as part of the larger aggrecan molecule. The large number of negatively charged CS chains on aggrecan draw water into the molecule, *via* a similar mechanism to HyA, which largely contributes to its swelling properties.<sup>166</sup> It is these unique swelling properties that allow articular cartilage to withstand repeated compressive loading so effectively.<sup>167</sup> The sulfate group on CS gives the molecule its negative charge and has also been shown to mediate interactions between CS and positively charged growth factors, such as TGF- $\beta$ .<sup>168,169</sup> Thus, CS contributes to both the mechanical and biological properties of articular cartilage. In the literature, CS has been reported to promote chondrogenesis by facilitating pre-cartilage condensation of MSCs, up-regulation of pro-chondrogenic genes and subsequent deposition of ECM components.<sup>170,171</sup> In addition to this, CS has also been shown to inhibit chondrocyte hypertrophy under dynamic loading conditions.<sup>172</sup> Therefore, it is not surprising that CS hydrogels have garnered attention in the field of TE for cartilage repair.

Although CS hydrogels are more popular in the formulation of injectable, gradient and photocrosslinkable hydrogels for cartilage repair,<sup>173–180</sup> they have also been used to formulate a number of biomimetic bioinks. When used in the formulation of bioinks, CS is typically included as part of a composite bioink and is often chemically modified with methacrylate (often referred to as CSMA)<sup>181,182</sup> or catechol<sup>183,184</sup> groups to improve bioink printability or adhesion to the cartilage defect *in vivo*. For example, Costantini *et al.* developed a cartilage ECM mimetic, crosslinkable bioink by blending alginate, GelMA and CS aminoethyl methacrylate which promoted chondrogenic differentiation of bone marrow-derived MSCs.<sup>181</sup> Abbadessa *et al.* also developed a thermo-sensitive and photocrosslinkable CSMA and poly(*N*-(2-hydroxypropyl) methacrylamide-mono/dilactate)-polyethylene glycol triblock copolymer

bioink with suitable 3D printing properties, and which also facilitated the fabrication of scaffolds with tailorable porosity that promoted chondrogenic cell proliferation.<sup>185</sup>

**3.1.4. Decellularised extracellular matrix bioinks for cartilage repair.** As discussed above, the mechanical and biological functions of native articular cartilage are highly dependent on the composition and complex biomaterial interactions within the tissue. In order to better mimic this intricate microenvironment, some researchers have opted to develop novel bioinks formulated from decellularised cartilage ECM (dECM). The ultimate goal when decellularising cartilage tissue is to remove all cellular material which may trigger adverse reactions *in vivo*, whilst simultaneously maintaining the ultrastructure and bioactivity of the tissue. There are a number of ways in which this may be achieved including the use of chemical agents, solvents, biologic agents or *via* physical means such as freeze-thaw, with each method presenting its own pros and cons.<sup>186,187</sup> As described by Crapo *et al.*, dECM should contain <50 ng double stranded DNA per mg ECM dry weight, <200 bp DNA fragment length and lack visible nuclear material when stained with 4',6-diamidino-2-phenylindole (DAPI) or haematoxylin and eosin (H&E) before being used for biomedical applications in order to minimise adverse reactions in the host.<sup>188</sup>

Cartilage tissue for formulating dECM-based bioinks is typically derived from porcine,<sup>189–192</sup> caprine<sup>193</sup> or bovine<sup>194</sup> sources. Following the removal of cellular material and sterilisation of the dECM to remove any pathogenic compounds, the dECM must then be further processed into a hydrogel formulation before being used as a bioink. This is usually achieved by freeze-drying the dECM, then blending or grinding the resulting lyophilate into small particles which can then be solubilised under acidic conditions using the enzyme pepsin.<sup>195</sup> Adjustment of the pH and salt concentration to physiological conditions then neutralises the pepsin and allows the formation of a dECM hydrogel which, similar to COL-I hydrogels, undergoes thermal crosslinking at 37 °C.<sup>189,195,196</sup> Therefore, similar to COL-I hydrogels, complete gelation can take up to 30 mins which poses problems for the mechanical stability of the 3D printed construct post-printing.

To overcome this issue, dECM hydrogels are often blended with other biomaterials when formulating bioinks for cartilage repair, which also has the added benefit of adding additional functionality to the bioink. Blending dECM with synthetic biomaterials such as polyvinyl alcohol (PVA) or PEG allows for the formulation of biomimetic bioinks with the bioactivity of native cartilage ECM, but with the enhanced printability and crosslinking control of a synthetically made bioink.<sup>193,197</sup> dECM has also been blended with silk fibroin to greatly improve its printability and fabricate structures which mimic the native architecture of cartilage tissue, and which can subsequently be crosslinked using 1-ethyl-3-(3-dimethylaminopropyl) carbodiimide (EDC)/*N*-hydroxysuccinimide (NHS).<sup>191</sup> Blending dECM hydrogels with a versatile biomaterial, such as alginate, allows formulation of bioinks with tune-



able stiffness and good printability.<sup>192</sup> dECM only or dECM composite bioinks can also be co-printed with polymers such as PCL to bring the mechanical properties of the 3D printed scaffold in line with those of native articular cartilage.<sup>191,192</sup> In the case of dECM only bioinks, co-printing with a polymer also provides mechanical scaffolding for the bioink during the 3D printing and crosslinking processes.<sup>191</sup>

Similar to other biomimetic biomaterials, dECM can also be chemically modified with methacrylate groups to confer crosslinking functionality and thus improve mechanical stability of the printed construct. For example, Visscher *et al.* formulated a methacrylated dECM hydrogel for auricular cartilage regeneration, which was blended with gelatin, HyA and glycerol to improve bioink printability and initial mechanical stability of the 3D printed construct. This bioink was shown to be more stiff and maintain a higher level of chondrocyte viability and proliferation than GelMA controls.<sup>190</sup> Overall, the inclusion of dECM in bioinks for cartilage repair has been shown to enhance the biocompatibility of the bioink and chondrogenesis of MSCs.<sup>189,191,197</sup> These bioinks can also be further functionalised to facilitate controlled release of bioactive factors, such as TGF- $\beta$ , to further increase expression of pro-chondrogenic genes and subsequent deposition of cartilage ECM components.<sup>192,193</sup>

**3.1.5. Interpenetrating network bioinks for cartilage repair.** As previously mentioned, the individual matrix components of articular cartilage play a synergistic role at a molecular level in the load-bearing and friction-reducing properties of the tissue. Therefore, when trying to mirror the properties of the native tissue and the microenvironment of the ECM, composite bioinks consisting of a network of two or more polymers can be more advantageous than bioinks consisting of a single polymer network. If a bioink consists of two individual crosslinked polymer networks that are physically entangled at a molecular level but still mutually independent from each other, it is referred to as an interpenetrating network (IPN).<sup>198</sup> IPNs consisting of two interpenetrating components with very different mechanical properties (e.g. one brittle and rigid, and one soft and ductile) are called double networks, and are of particular interest in this field due to the fact that native cartilage ECM is innately composed of double networks.<sup>199</sup> IPN bioinks differ from conventional composite bioink formulations in that the individual polymers that make up the bioink matrix cannot be separated from each other without breaking crosslinks.<sup>200</sup> An example of such a bioink would be a GelMA and alginate bioink formulation, similar to that formulated by Wang *et al.*,<sup>148</sup> which can be photocrosslinked and then subsequently ionically crosslinked. This facilitates the fabrication of a scaffold whereby the two composite polymers are interlocked at a molecular level, but not actually chemically bonded to each other.

IPN bioinks offer several advantages over single polymer network bioinks or non-IPN composite bioinks in the field of cartilage TE. One such advantage is that IPN bioinks have enhanced compressive stiffness and toughness when compared to the individual biomaterial components that make up

the bioink.<sup>201</sup> For example, an alginate and polyacrylamide IPN hydrogel formulated by Liao *et al.* was found to have a compressive modulus approximately four times greater than its individual biomaterial counterparts.<sup>202</sup> Similarly, Li *et al.* found that the equilibrium modulus of a gellan gum and PEG diacrylate (PEGDA) double network IPN was approximately 10 times higher than that of the respective constituent hydrogels.<sup>203</sup> Thus, IPN bioinks can be tailored to mimic the mechanical stiffness of articular cartilage ECM, without significantly increasing the polymer concentration or crosslink density. This is beneficial for TE applications as high polymer concentrations or crosslink densities can hinder cell migration and attachment, as well as diffusion of nutrients and waste products.

Another advantage of IPN bioinks is the ability to tune material properties, such as viscoelasticity or stiffness, in an independent manner in order to influence cell behaviour.<sup>200</sup> This fine control of the bioink microenvironment is desirable as it has been shown that the mechanical and rheological properties of a cell's environment have a significant influence on cell spreading, proliferation and differentiation.<sup>204–207</sup> For example, Lee *et al.* demonstrated that chondrocytes embedded in fast relaxing viscoelastic alginate hydrogels undergo higher levels of proliferation and produce a more extensive and interconnected ECM than those embedded in slow relaxing hydrogels.<sup>208</sup> Park *et al.* also demonstrated that MSCs cultured on stiffer substrates were more likely to differentiate into smooth muscle cells, while MSCs cultured on softer substrates tended towards a chondrogenic or adipogenic lineage (dependent on the presence or absence of TGF- $\beta$ ).<sup>205</sup> This alludes to the critical role that bioink properties play in regulating chondrocyte behaviour and thus the ability to control these parameters is highly desirable in the formulation of bioinks for cartilage repair.

A number of research groups have employed IPNs of natural and synthetic biomaterials to formulate bioinks for cartilage repair with enhanced mechanical properties, biocompatibility and chondrogenic potential. Wang *et al.* and Schipani *et al.* both developed alginate and GelMA-based IPN bioinks, which were shown to possess superior mechanical properties to their constituent hydrogel components and promoted chondrogenesis of MSCs and subsequent deposition of articular cartilage ECM components.<sup>124,148</sup> Wu *et al.* designed a double network IPN bioink composed of gellan gum and PEGDA which had desirable 3D printing properties and could undergo non-covalent and covalent crosslinking post-printing respectively to fabricate scaffolds with versatile mechanical properties.<sup>209</sup> Ni *et al.* optimised a double network bioink consisting of silk fibroin and hydroxyl propyl methyl cellulose methacrylate (HPMC-MA), whereby silk fibroin  $\beta$ -sheets formed the more brittle primary network and photocrosslinked HPMC-MA formed the ductile secondary network. Formation of the double network improved the mechanical properties of the bioink and the bioink was also shown to facilitate proliferation and chondrogenesis of MSCs.<sup>210</sup> Thus, this demonstrates that a wide range of biomaterial properties



can be synergistically combined through the fabrication of these biomimetic networks.

The main advantages and disadvantages of each bioink type outlined above are summarised in Table 1 below.

### 3.2. Functionalising 3D printed scaffolds for cartilage repair with cells

Complete regeneration of functional cartilage tissue requires mature chondrocytes which are capable of producing a collagen type II and GAG-rich ECM to gradually replace the implanted TE scaffold. In the field of TE for cartilage repair, there are two ways in which cells may be incorporated into the scaffold. The first method involves implanting a cell-free scaffold with sufficient porosity into the cartilage defect and allowing the patient's own cells to infiltrate the scaffold and lay down their own ECM.<sup>43</sup> The second method involves functionalising a bioink with cells which have been harvested from the patient and expanded *in vitro*, and subsequently 3D printing a scaffold embedded with the patient's expanded cells in a process known as '3D bioprinting'.<sup>5</sup> However, 3D bioprinting scaffolds for cartilage repair is not without its challenges. Thus, the following sections will discuss the considerations that should be taken into account when formulating cell-laden bioinks for 3D bioprinting scaffolds for cartilage repair.

**3.2.1. Selecting a cell type for cartilage bioprinting.** As previously discussed, MSCs have the ability to differentiate into chondroprogenitor cells and chondrocytes when provided with the appropriate biological and physical cues, and thus any of these cell types can be used for cartilage TE. However, regardless of the cell type selected, two main challenges remain when incorporating cells into bioinks for cartilage repair. The first is maintaining the viability of cells following exposure to significant shear stress during the 3D printing process, and the second challenge is ensuring that the cells differentiate into, and/or maintain, an articular chondrocyte phenotype. With regards maintaining cell viability, the bioink can provide protection to the encapsulated cells against shear stress if it is not too viscous itself,<sup>5</sup> and thus most studies report post-printing cell viability levels in excess of 80%, regardless of cell type.<sup>99,104,143,214</sup> Maintaining an articular chondrocyte phenotype is essential to prevent the formation of mechanically inferior fibrocartilage and to ensure that the cells do not become hypertrophic, and this can be controlled through careful selection of biomaterials and providing the cells with the correct biological cues.

MSCs are one of the most popular cell types used in cartilage TE due to their proliferative and differentiation abilities, and are usually obtained from bone marrow or adipose tissue.<sup>218,219</sup> In fact, MSCs are currently employed clinically to promote cartilage regeneration as part of the microfracture surgical procedure, during which tiny fractures are made in the subchondral bone allowing the release of bone marrow MSCs into the defect which ultimately develop into fibrocartilage.<sup>13</sup> There are extensive reports in the literature that show that MSCs from human,<sup>104,123,192,215,220</sup> rat,<sup>221,222</sup> bovine,<sup>157</sup>

rabbit<sup>223,224</sup> and porcine<sup>124,192</sup> sources can be successfully directed towards a chondrogenic lineage when encapsulated within a suitably formulated biomimetic bioink. For example, Rathan *et al.* reported that MSCs encapsulated in a dECM-functionalised alginate bioink expressed higher levels of the pro-chondrogenic genes Col2a1 and ACAN than those encapsulated in the non-functionalised alginate control. However, gene expression of Col1a1 and RUNX2 was also elevated, suggesting that a proportion of MSCs had also followed an endochondral or osteogenic pathway.<sup>192</sup> This highlights the importance of bioink design when attempting to direct the differentiation of MSCs.

Articular chondroprogenitor cells (ACPCs) can also be used to functionalise bioinks for cartilage repair, and similar to MSCs, have been shown to produce a collagen type II and GAG rich matrix when encapsulated within biomimetic bioinks.<sup>214,225,226</sup> ACPCs can be more advantageous than MSCs in the field of TE for cartilage repair as they have already started on a chondrogenic pathway and express high levels of SOX-9, also known as the master regulator of chondrogenesis.<sup>227,228</sup> Similar to MSCs, ACPCs also have a good proliferative capacity, are capable of migration and express similar cell surface markers.<sup>229</sup>

Mature chondrocytes from human, porcine, rabbit, bovine and equine sources have also been successfully shown to produce articular cartilage-like ECM components in biomimetic 3D bioprinted scaffolds for cartilage repair.<sup>99,124,143,212,230–232</sup> However, the main drawback with using mature articular chondrocytes is that availability of tissue from which to isolate these cells is limited and the tissue that can be harvested contains quite a low density of chondrocytes.<sup>233</sup> Mature chondrocytes also have a tendency to undergo dedifferentiation when cultured *in vitro*, as is often seen following the autologous chondrocyte implantation procedure (ACI).<sup>234</sup> However, similar to MSCs, this risk can be reduced by providing the cells with the correct biological and physical cues through appropriate selection of biomaterials and/or inclusion of bioactive factors, in order to maintain an articular cartilage phenotype.

**3.2.2. Selecting a cell density for cartilage bioprinting.** Having selected a cell type to incorporate into the bioink, the next step is to decide on a suitable cell density for the bioink, and this is usually expressed as the number of cells in millions (M) per millilitre (mL) of bioink. In healthy articular cartilage of the human femoral condyle, the density of chondrocytes within the tissue varies with distance from the articular surface, ranging from approximately 24 000 cells per mm<sup>3</sup> in the superficial zone, to 10 000 cells per mm<sup>3</sup> in the middle zone, to 7000 cells per mm<sup>3</sup> in the deep zone.<sup>235</sup> In bioprinting terms, this is equivalent to approximately 24M cells per mL in the superficial zone, 10M cells per mL in the middle zone and 7M cells per mL in the deep zone. Therefore, the majority of bioinks for cartilage repair are functionalised with MSCs,<sup>123,157,210,221–224</sup> ACPCs,<sup>225,226</sup> mature articular chondrocytes,<sup>212,230,236</sup> or co-cultures of MSCs and chondrocytes<sup>124,232</sup> at cell densities of 5M to 20M cells per mL



**Table 1** A summary of the key advantages and disadvantages of popular biomimetic biomaterials used to formulate bioinks for cartilage repair

Category	Biomaterial	Concentrations used	Crosslinking method	Key Advantages	Key Disadvantages	Ref.
Collagen	Collagen type I	0.5–5%	Thermal crosslinking	Good cell viability (>80%) post-printing and contains RGD cell-binding motif	Hydrogels can be mechanically weak and thermal crosslinking process is difficult to control. Must be printed at low temperatures (2–8 °C)	99, 108 and 211–213
	Methacrylated collagen	0.3%	Thermal and photo-crosslinking	Good cell viability (>80%) post-printing and contains RGD cell-binding motif. Improved mechanical properties <i>versus</i> unmodified collagen type I bioinks	Must be printed at low temperatures (2–8 °C). Use of UV light during photo-crosslinking may have negative effects on cell viability	104
	Gelatin	4.5–10% (as part of a composite bioink)	Not readily crosslinkable	Good cell viability (>90%) post-printing and contains RGD cell-binding motif. Already has US FDA approval for use in the biomedical industry	Not readily crosslinkable for 3D printing purposes in its unmodified state. Low viscosity at body temperature	115–117, 214 and 215
	Methacrylated gelatin	5–30%	Photo-crosslinking	Good cell viability (>80%) post-printing and contains RGD cell-binding motif. Improved mechanical properties <i>versus</i> unmodified gelatin bioinks	Use of UV light during photo-crosslinking may have negative effects on cell viability	119–126 and 216
Glycosaminoglycan	Hyaluronic acid	1–30% (as part of a composite bioink)	Not readily crosslinkable	Good cell viability (>80%) post-printing and contains CD44 cell-binding domain. Plays important role in the biological and mechanical properties of articular cartilage	Not readily crosslinkable for 3D printing purposes in its unmodified state. Poor print resolution unless blended with other biomaterials or chemically modified	143–147
	Methacrylated hyaluronic acid	0.5–4%	Photo-crosslinking	Good cell viability (>80%) post-printing and contains CD44 cell-binding domain. Improved mechanical properties <i>versus</i> unmodified hyaluronic acid hydrogels	Higher degrees of functionalisation can negatively affect CD44 cell-binding and chondrogenesis	123, 142 and 151–156
	Chondroitin sulfate	1–10% (as part of a composite bioink)	Not readily crosslinkable	Good cell viability (>90%) post-printing. Plays important role in the biological and mechanical properties of articular cartilage	Not readily crosslinkable for 3D printing purposes in its unmodified state. Poor print resolution unless blended with other biomaterials or chemically modified	217
	Chondroitin sulfate methacrylate	2–4% (as part of a composite bioink)	Photo-crosslinking	Good cell viability (>80%) post-printing. Improved mechanical properties <i>versus</i> unmodified chondroitin sulfate hydrogels	Often required to be formulated as part of a composite bioink to improve printability	181, 182 and 185
	Decellularised ECM	0.2–20%	Thermal crosslinking	Good cell viability (>70%) post-printing. Possesses bioactivity of several biomaterials native to articular cartilage. Can be chemically modified to confer crosslinking functionality and improve printability	Thermal crosslinking of hydrogels can take up to 1 h at 37 °C and is a difficult process to control. Poor print resolution unless blended with other biomaterials, chemically modified or printed using a support bath	190–193 and 197
Composite	Interpenetrating networks	—	—	Have enhanced compressive stiffness and toughness when compared to the individual biomaterial components that make up the bioink. Ability to tune material properties, such as viscoelasticity or stiffness, in an independent manner in order to influence cell behaviour. Can possess bioactivity of several biomaterials native to articular cartilage	Disadvantages dependent on biomaterial selection	124, 148, 202, 203, 209 and 210

to mimic the native cellular composition of human articular cartilage.

However, studies have also been conducted to investigate the effects of low cell densities, in the range of 1 to 2M cells per mL, on chondrogenesis in 3D bioprinted scaffolds. Henrionnet *et al.* fabricated scaffolds using an alginate, gelatin and fibrinogen bioink, functionalised with MSCs at two respective cell densities – 1M cells per mL and 2M cells per mL. Interestingly, following 28 days culture in TGF- $\beta$ 1 supplemented media, scaffolds containing the lower cell density showed more enhanced expression of the chondrogenic markers Col2a1, ACAN and SOX-9.<sup>215</sup> Similarly, Koo *et al.* 3D bioprinted a collagen-based scaffold containing rabbit articular chondrocytes at a density of 1M cells per mL which successfully facilitated neo-cartilage formation in osteochondral defects of the rabbit knee.<sup>99</sup> Thus, when provided with a suitable micro-environment, low cell densities can also be used to promote cartilage tissue regeneration.

**3.2.3. Incorporating bioactive factors into 3D printed scaffolds for cartilage repair.** The term 'bioactive factors' typically refers to mineral ions, growth factors (GFs) or intracellular signalling molecules and recent research in the field of TE has recognised the significant role played by these factors in the regeneration of cartilage and bone tissue.<sup>237</sup> It has been widely reported that pro-osteogenic factors such as bone morphogenetic protein 2 (BMP-2)<sup>50,238–241</sup> and transforming growth factor  $\beta$  (TGF- $\beta$ )<sup>242</sup> as well as pro-angiogenic factors such as vascular endothelial growth factor (VEGF)<sup>239,241,243</sup> and platelet-derived growth factor (PDGF)<sup>244</sup> have been used to promote bone regeneration. Likewise, the critical role played by the TGF- $\beta$  superfamily and the SOX family of transcription factors (SOX-5, SOX-6 and SOX-9 – known as the SOX-Trio), amongst others, in promoting chondrogenesis and suppressing hypertrophy has also been recognised.<sup>245,246</sup> As these bioactive factors are key in the formation of articular cartilage, it makes logical sense to exploit these factors to mimic naturally occurring pro-chondrogenic cues in 3D printed scaffolds for cartilage repair.

Due to the pivotal role that GFs play in promoting proliferation and chondrogenic differentiation of MSCs during long bone formation, they are the most common bioactive factor used to functionalise 3D printed scaffolds for cartilage repair. A number of growth factor families have attracted interest in the field of TE for cartilage repair. The TGF- $\beta$  family are known promoters of chondrogenesis, however TGF- $\beta$ 1 and 3 in particular has been shown to elicit a strong chondrogenic response during *in vitro* and *in vivo* studies.<sup>247–250</sup> Thus, these TGF- $\beta$  isoforms are particularly popular in the field of 3D printing for cartilage repair, both as a supplement for chondrogenic cell media and as a bioink component to enhance chondrogenesis of MSCs.<sup>148,192,193,223,251–253</sup> The BMP family are a subgroup of the TGF- $\beta$  superfamily that have been shown to regulate almost every step of the chondrogenic pathway. Of particular relevance to cartilage repair, BMP-2, 4 and 7 promote MSC condensation at the beginning of the chondrogenic pathway, as well as promoting chondrogenic differen-

tiation of chondroprogenitor cells by maintain the expression of the pro-chondrogenic SOX transcription factors.<sup>76,254</sup> Similar to TGF- $\beta$ , BMPs can also be added to bioinks for osteochondral repair.<sup>255</sup>

Platelet-rich plasma (PRP) is also used as a source of endogenous GFs for cartilage TE. PRP is obtained by centrifuging a sample of peripheral blood to create a concentrated pellet of platelets, which release proteins and GFs following activation.<sup>256</sup> GFs obtained from platelets include IGF-1, PDGF, TGF- $\beta$ 1 and basic fibroblast growth factor (bFGF), amongst others, and intra-articular injections of PRP have been shown to promote the repair of smaller cartilage defects in clinical studies.<sup>257–259</sup> Thus, a number of recent studies have attempted to harness the chondrogenic potential of PRP by incorporating it into 3D printed scaffolds for cartilage repair.<sup>221,260–262</sup> For example, Irmak *et al.* developed a patient-specific photo-activated PRP and GelMA bioink which facilitated the controlled release of the GFs PDGF, TGF- $\beta$ 1 and bFGF, and enhanced the expression of pro-chondrogenic genes and deposition of articular cartilage matrix components.<sup>260</sup> The platelets adhered to the GelMA-based bioink *via* integrin receptors and were activated upon exposure to near-infrared light, allowing for the controlled release of GFs. Similarly, Luo *et al.* incorporated freshly activated PRP into a 3D bioprinted MSC-laden GelMA scaffold and implanted it intramuscularly into a mouse. They found that addition of the PRP promoted chondrogenic differentiation of the embedded MSCs and deposition of articular cartilage-specific ECM components.<sup>221</sup>

**3.2.4. Cell aggregates, micro-tissues and organoids as bioink alternatives.** Although not within the scope of this review, it is worth noting that a number of 'scaffold-free' approaches to regenerating cartilage tissue have recently come to the fore in this field. These approaches typically involve generating precursor tissues *in vitro* which are already committed to a chondrogenic lineage, and then implanting these tissues *in vivo* to promote healing of articular cartilage defects.<sup>263</sup> These cellular aggregates, micro-tissues and organoids can also be 3D bioprinted into more complex structures using a variety of techniques, and thus a biomaterial scaffold may not be required to support the growth of the new tissue.<sup>264</sup> These cellular building blocks can also be used in tandem with more traditional biomaterial-based TE approaches in a process known as modular assembly.<sup>265</sup> An extensive review of this topic is outlined by Burdis *et al.*<sup>263</sup>

### 3.3. Gradient 3D printed scaffolds for cartilage repair

In recent years, there has been a growing acceptance within the field of TE for cartilage repair that homogenous biomaterial scaffolds with a uniform architecture and composition are not well positioned to mirror the complexity and functionality of the native tissue. This is where 3D printing has really come into its own, allowing researchers to fabricate gradient scaffolds whose structure and composition mimic the zonal architecture of articular cartilage. Gradients within 3D printed scaffolds can be achieved by creating zonal differences in parameters such as biomaterial composition, pore size, cell density



or presence of bioactive factors to promote deposition of zone-specific matrix components. Some examples of 3D printed gradient scaffolds for cartilage repair are outlined below.

**3.3.1. Biomaterial gradients.** Biomaterial gradients within a 3D printed scaffold for cartilage repair can be used to induce zonal production of matrix components by embedded cells. For example, Zhang *et al.* 3D printed a gradient osteochondral scaffold consisting of a hydrogel cartilage layer, a 60%/40% hydrogel and nanohydroxyapatite calcified cartilage layer and a 30%/70% subchondral bone layer. Following 12 weeks implantation in osteochondral defects of the rat knee, the gradient scaffolds demonstrated superior healing to the non-gradient control scaffolds and a zonal organisation of cells and cartilage and bone matrix components was evident throughout the defect site.<sup>266</sup>

**3.3.2. Pore size and architecture gradients.** The pore architecture and specifically pore size of a TE scaffold has long been known to influence cell attachment and differentiation,<sup>43</sup> and some recent studies have exploited this to promote zonal differentiation of cells within 3D printed gradient scaffolds. For example, Sun *et al.* 3D printed a composite scaffold using PCL and a MSC-laden hydrogel which had a pore size gradient ranging from 150  $\mu\text{m}$  in the superficial layer to 750  $\mu\text{m}$  in the deep layer. They reported that cells cultured in the superficial layer displayed a more articular chondrocyte phenotype, as determined by the expression of Col2a1 and deposition of GAGs, while cells in the deep layer displayed a more hypertrophic phenotype, as determined by the expression of Col10a1.<sup>267</sup> Similarly, Cao *et al.* used PCL and to 3D print a scaffold framework with a gradient architecture and pore size ranging from 300  $\mu\text{m}$  in the superficial zone to 700  $\mu\text{m}$  in the deep zone. When a MSC-laden alginate-based hydrogel was cast into the PCL framework, cells in the gradient scaffold produced higher levels of articular cartilage matrix components than those in non-gradient scaffold controls following three weeks in culture.<sup>268</sup>

**3.3.3. Cell density gradients.** Several research groups have designed multi-layered scaffolds for cartilage repair with cell density gradients that match the zonal gradient of the native tissue, as outlined in section 3.2. For example, Ren *et al.* 3D bioprinted a collagen type II chondrocyte-laden scaffold with a cell density gradient ranging from 21M cells per mL in the superficial zone, to 14M cells per mL in the middle zone and 7M cells per mL in the deep zone (a 3:2:1 ratio). They found that ECM production was positively correlated with cell density and that there was zonal differences in ECM properties based on cell density, similar to those seen in the native tissue.<sup>236</sup> Similarly, Dimaraki *et al.* 3D bioprinted PCL-reinforced alginate-based zonal scaffolds containing human chondrocytes at a density of 20M cells per mL in the superficial zone, 10M cells per mL in the middle zone and 5M cells per mL in the deep zone. They found that distinct zonal cell densities could be partially maintained over a 25 day culture period and that, similar to Ren *et al.*, creating a cell density gradient resulted in gradient deposition of cartilage ECM components.<sup>269</sup>

**3.3.4. Cell type gradients.** When 3D bioprinting cell-laden scaffolds for cartilage repair, there is evidence to suggest that using more than one cell type can help create a zonal gradient and promote articular cartilage matrix production. For example, Levato *et al.* found that MSCs synthesised the highest levels of cartilage matrix, followed by ACPCs, followed by mature chondrocytes, when encapsulated within a GelMA hydrogel. However, despite outperforming ACPCs in matrix production, MSCs expressed much more of the hypertrophic marker Col10a1 than ACPCs, while ACPCs produced the highest levels of the lubricin gene, PRG4. Due to this difference in gene expression, the authors decided that when 3D bioprinting a bi-layered scaffold for cartilage repair, MSCs were more suitable in the middle/deep zone layer, while ACPCs were more suitable in the superficial layer.<sup>225</sup> This allowed for the fabrication of an articular cartilage mimetic scaffold with distinct cellular and ECM distribution. There is also evidence to suggest that co-cultures of MSCs and mature chondrocytes help to support more robust chondrogenesis and prevent expression of hypertrophic markers within biomimetic 3D bio-printed scaffolds.<sup>124,232</sup>

**3.3.5. Bioactive factor gradients.** Bioactive factor gradients can also be incorporated into 3D printed scaffolds for cartilage repair to promote zonal differentiation of embedded cells. Sun *et al.* employed this approach to 3D print a gradient scaffold which contained TGF- $\beta$ 3-laden PLGA microspheres in the superficial and middle zones of the scaffold, and BMP-4-laden PLGA microspheres in the deep zone. Following 12 weeks implantation in cartilage defects of the rabbit knee, the controlled release of TGF $\beta$ -3 and BMP-4 induced zonal expression of PRG4, aggrecan, and collagen types II and X, resembling native articular cartilage.<sup>223</sup>

## 4. Bioink formulation – what works best?

Thus far in this review we have discussed how a variety of different biomimetic biomaterials, cell types and densities, and bioactive factors can be used to formulate bioinks for cartilage repair. In doing so, we have highlighted a number of biomimetic bioink formulations, each of which possesses desirable 3D printing properties, biocompatibility and chondrogenic potential. However, clear evidence is yet to accrue on which bioink formulation works best. Although it is a relatively simple and logical question to pose, differences in experimental procedures make it difficult to draw direct comparisons between studies.

Despite this fact, several formulation trends can still be observed across studies. With regards biomaterial composition of bioinks, the majority of studies use composite bioinks consisting of two or more biomaterial components. In these studies, one of these components is often a GAG-derived (*e.g.* a HyA-derived biomaterial) or a GAG-mimetic (*e.g.* alginate) biomaterial, while the other is a collagen-derived (*e.g.* gelatin or GelMA) biomaterial. At least one of these biomaterial com-



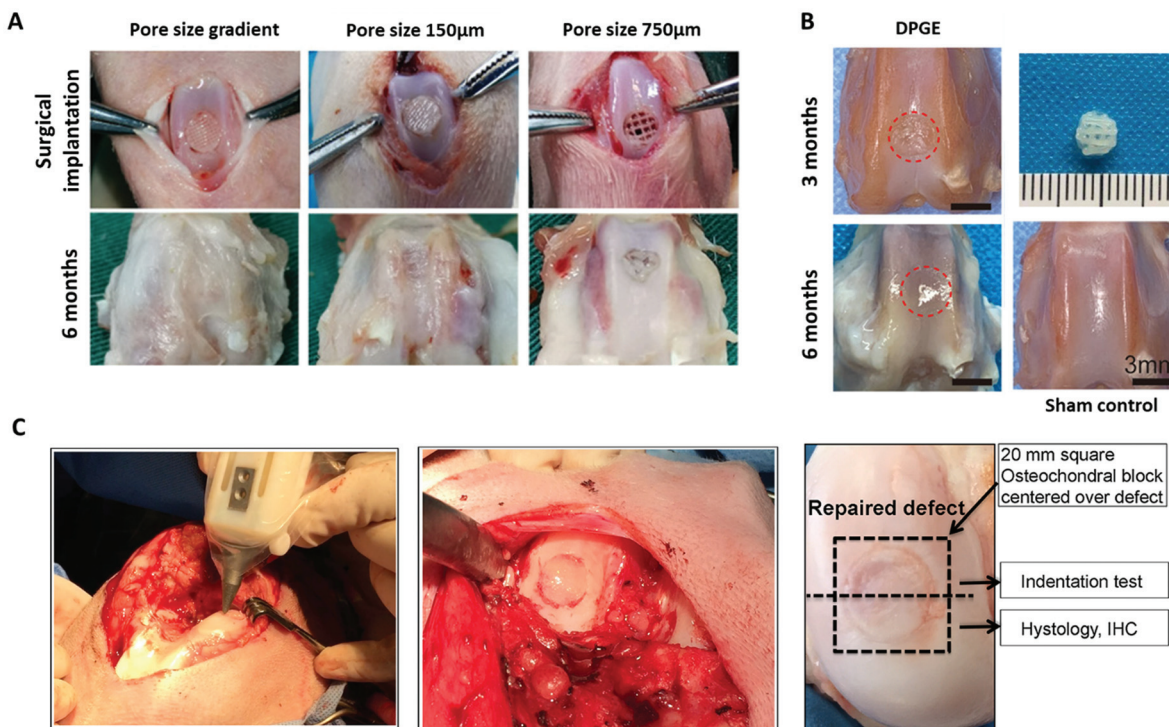


**Fig. 5** 3D bioprinted biomimetic scaffolds for cartilage repair have been shown to facilitate regeneration of articular cartilage *in vivo*. (A) Surgical implantation of a PCL-reinforced gelatin, fibrinogen, HA and glycerol with a pore size gradient (ranging from 150  $\mu\text{m}$  in superficial zone to 750  $\mu\text{m}$  in the deep zone). Following 6 months implantation, the gradient scaffolds displayed better tissue repair than the non-gradient scaffolds in chondral defects of the rabbit knee. (B) Repair of articular cartilage 3 months and 6 months post-implantation of a 3D bioprinted PCL-reinforced aptamer-functionalised GelMA and dECM scaffold. (C) *In situ* 3D bioprinting of a scaffold for cartilage repair using a GelMA and MeHA MSC laden bioink in a chondral defect of the sheep knee, and subsequent repair of the defect following implantation for 2 months. A is re-printed and adapted from Sun *et al.*<sup>267</sup> with permission from Elsevier (Copyright © 2021, Elsevier B.V.), B is re-used and adapted with permission from Yang *et al.*<sup>270</sup> (Copyright © 2021, American Chemical Society), and C is re-used and adapted with permission from Di Bella *et al.*<sup>271</sup> (Copyright © 2017, John Wiley & Sons, Ltd).

ponents also possesses crosslinking functionality. With regards the cellular composition of these bioinks, the use of MSC and/or chondrocyte-laden bioinks is more popular than ACPC-laden bioinks. However, regardless of the cell type used, higher cell densities (in the range of 10 to 20M cells per mL) are more commonly employed when a single cell density is present throughout the entire 3D bioprinted scaffold. Where a cell density gradient is employed in a 3D bioprinted scaffold, it generally mirrors that found in native articular cartilage, *i.e.* approximately 20M mL<sup>-1</sup> in the superficial zone, 10M mL<sup>-1</sup> in the middle zone and 5M mL<sup>-1</sup> in the deep zone.

Investigation of the composition of 3D printed scaffolds used in successful *in vivo* studies also indicates which bioink formulations achieve functional regeneration of articular cartilage in a living, moving organism. These scaffolds are usually 3D printed *ex vivo* and surgically implanted into the cartilage defect, however in some instances the scaffold may be 3D printed *in situ* directly into the defect (Fig. 5C).<sup>270,271</sup> Similar to *in vitro* studies, it is difficult to draw direct comparisons between the results of *in vivo* studies due to differences in animal models used and experimental design.<sup>272</sup> However, similar to above, there are formulation trends present across studies. Firstly, in a large number of successful *in vivo* studies,

the bioink (either composite or single component) is co-printed with a polymer to improve the mechanical properties of the 3D printed scaffold<sup>99,125,223,267,270,273,274</sup> (Fig. 5B). These polymers are usually thermoplastics with relatively low melting points, such as PCL. Secondly, gradient 3D printed scaffolds are frequently used to promote chondral or osteochondral zonal differentiation of cells and deposition of ECM components (*e.g.* pore size gradient, as shown in Fig. 5A).<sup>267</sup>

## 5. Future perspectives

From its inception with the development of the first TE biomaterial-based scaffolds for skin repair in the 1970s and 1980s, TE has positioned itself as having immense potential in the field of modern medicine.<sup>275</sup> The advent of 3D printed scaffolds has further advanced this field, allowing for the fabrication of complex biomimetic biomaterial structures with defined architecture, which can be functionalised with cells and bioactive factors in a manner that mimics the native tissue. However, the question still remains – how can the gap between bench and bedside, which currently hinders the clin-



cal use of 3D printed scaffolds for the treatment of cartilage defects, finally be bridged? The answer to this question may lie in the field of gene therapy.

Gene therapy involves the introduction of a specific genetic sequence into a cell *via* complexation with a targeted delivery vector in order to introduce a new gene, or promote or silence expression of a pre-existing gene. This, in turn, leads to an increase or decrease in the expression of a particular protein of interest. At the beginning the century, the field of gene therapy suffered a severe setback following reports of severe side-effects and deaths in clinical trials for gene therapeutic treatments of X-linked severe combined immunodeficiency (SCID) and ornithine transcarbamylase deficiency respectively.<sup>276</sup> However, in recent years a range of gene therapeutics have been granted marketing authorisations worldwide for the treatment of a number of orphan diseases and cancers, amongst other conditions.<sup>277</sup> In the last year, in particular, the field of gene therapy has been catapulted into the lime-light following the successful development and regulatory approval of two messenger RNA (mRNA)-based vaccines against SARS-CoV-2 (also known as Covid-19); the mRNA-1273 SARS-CoV-2 vaccine,<sup>278</sup> and the BNT162b2 mRNA Covid-19 vaccine<sup>279</sup> (colloquially known as the 'Moderna' and 'Pfizer/BioNTech' vaccines respectively). Both of these vaccines contain mRNA encoding for the SARS-CoV-2 spike protein which is encapsulated in lipid nanoparticles to enable uptake by cells, subsequently leading to expression of the spike protein, followed by the desired immune response.<sup>280</sup>

Aside from mRNA, other examples of genetic sequences which can be introduced into cells include pDNA, miRNA and silencing RNA (siRNA), amongst others.<sup>281</sup> Delivery vectors used to transport these genetic sequences into the cell can be viral or non-viral in nature. Lentiviral and adeno-associated viral vectors are the most commonly used viral vectors in the field of gene therapy and although they exhibit high transfection efficiency, safety concerns such as insertional mutagenesis have traditionally hindered their clinical use.<sup>276,282,283</sup> Therefore, non-viral delivery vectors including layered double hydroxides (LDHs),<sup>284</sup> lipid-based vectors such as Lipofectamine,<sup>285</sup> polymers such as polyethylenimine (PEI),<sup>286</sup> inorganic nanoparticles such as nanohydroxyapatite (nHA)<sup>240</sup> and cell-penetrating peptides (CPPs) such as the RALA amphiphatic peptide<sup>287</sup> and glycosaminoglycan binding enhanced transduction (GET) peptides<sup>288</sup> are becoming increasingly popular in this field. Our own research group has been pioneering the concept of gene-activated TE scaffolds for a myriad of applications including cartilage repair,<sup>245</sup> bone repair,<sup>241,286,289</sup> skin repair<sup>290-292</sup> and peripheral nerve repair.<sup>293</sup>

Incorporating these gene therapeutic nanoparticles into bioinks for cartilage repair would allow for the fabrication of multi-layered scaffolds with distinct zonal biological cues. While this approach has been taken with the use of GFs, their release from 3D printed scaffolds can be difficult to control and can result in off-target side-effects.<sup>276</sup> Thus, gene therapy

can be used to promote the expression of pro-chondrogenic factors *in vivo* without the risk of adverse effects. The concept of gene-activation of bioinks was pioneered by members of our group, Gonzalez-Fernandez *et al.*, who developed a MSC-laden, pore-forming alginate-based bioink which facilitated the controlled release of RALA and pDNA gene therapeutic nanoparticles. This bioink was used to 3D print a PCL-reinforced gradient scaffold for osteochondral repair which contained nanoparticles consisting of RALA and pDNA for TGF- $\beta$ 3, BMP-2 and SOX-9 respectively in the cartilage layer, and nanoparticles consisting of nHA and pDNA for BMP-2 in the bone layer. In an *in vivo* mouse model, these bi-layered gene-activated scaffolds facilitated the production of a bone layer, overlaid with a collagen type II and GAG-rich articular cartilage layer.<sup>50</sup>

Therefore, the development of these novel bioinks is building on recent successes in the fields of TE and gene therapy to deliver next generation 3D printed gene-activated scaffolds. These gene-activated scaffolds could potentially bridge the aforementioned gap between the bench and bedside, leading to a novel clinical treatment for a myriad of conditions including chondral and osteochondral defects, skin wounds and spinal cord injury, to name a few. Thus, this field has the potential to greatly improve quality of life for patients worldwide.

## 6. Conclusion

To conclude, the development of TE scaffolds, which are 3D printed using biomimetic bioinks functionalised with cells and bioactive factors or gene therapeutics, may finally offer the opportunity to develop scaffolds which fully recapitulate the complex zonal architecture of native articular cartilage and thus increase the likelihood of an effective clinical treatments for cartilage repair. The ability to restore functionality to the articular joints of patients would have a profound effect on the quality of life of millions of patients worldwide.

## Author contributions

DOS, CC and FOB devised the structure of the manuscript, and DOS drafted and wrote the manuscript. DOS created figures used unless otherwise stated. DOS, CC, and FOB revised the manuscript critically and suggested references. CC and FOB supervised the project and FOB provided funding for the project. All authors have read and approved the final submitted manuscript.

## Conflicts of interest

The authors have no conflicts of interest to declare.



## Acknowledgements

The authors acknowledge funding from the European Research Council under the European Community's Horizon 2020 research and innovation programme under ERC Advanced Grant agreement n°788753 (ReCaP). Dr. Curtin acknowledges funding from the Health Research Board (HRB) in Ireland under grant agreement ILP-POR-2019-023. All original figures were created with Biorender.com.

## References

- 1 J. F. V. Vincent, O. A. Bogatyreva, N. R. Bogatyrev, A. Bowyer and A.-K. Pahl, *J. R. Soc., Interface*, 2006, **3**, 471–482.
- 2 J. M. Benyus, *Biomimicry: Innovation Inspired by Nature*, William Morrow & Company, 1997.
- 3 F. J. O'Brien, *Mater. Today*, 2011, **14**(3), 88–95.
- 4 C. M. Curtin, J. C. Nolan, R. Conlan, L. Deneweth, C. Gallagher, Y. J. Tan, B. L. Cavanagh, A. Z. Asraf, H. Harvey, S. Miller-Delaney, J. Shohet, I. Bray, F. J. O'Brien, R. L. Stallings and O. Piskareva, *Acta Biomater.*, 2018, **70**, 84–97.
- 5 W. Sun, B. Starly, A. C. Daly, J. A. Burdick, J. Groll, G. Skeldon, W. Shu, Y. Sakai, M. Shinohara, M. Nishikawa, J. Jang, D.-W. Cho, M. Nie, S. Takeuchi, S. Ostrovidov, A. Khademhosseini, R. D. Kamm, V. Mironov, L. Moroni and I. T. Ozbolat, *Biofabrication*, 2020, **12**, 022002.
- 6 R. Chaudhuri, M. Ramachandran, P. Moharil, M. Harumalani and A. K. Jaiswal, *Mater. Sci. Eng., C*, 2017, **79**, 950–957.
- 7 M. Lemoine, S. M. Casey, J. M. O'Byrne, D. J. Kelly and F. J. O'Brien, *Biochem. Soc. Trans.*, 2020, **48**(4), 1443–1445.
- 8 S. MacNeil, *Mater. Today*, 2008, **11**(5), 26–35.
- 9 J. F. Mano and R. L. Reis, *J. Tissue Eng. Regener. Med.*, 2007, **1**, 261–273.
- 10 R. Wittenauer, L. Smith and K. Aden, *Background Paper 6.12 Osteoarthritis*, 2013. Available from: [https://www.who.int/medicines/areas/priority\\_medicines/BP6\\_12Osteo.pdf](https://www.who.int/medicines/areas/priority_medicines/BP6_12Osteo.pdf) [Accessed on 18/02/21].
- 11 WHO Department of Chronic Diseases and Health Promotion, *Chronic rheumatic conditions*, 2021. Available from: <https://www.who.int/chp/topics/rheumatic/en/> [Accessed on 18/02/21].
- 12 B. S. Dunkin and C. Lattermann, *Operative Techniques in Sports Medicine*, 2013, vol. 21, pp. 100–107.
- 13 J. R. Steadman, B. S. Miller, S. G. Karas, T. F. Schlegel, K. K. Briggs and R. J. Hawkins, *J. Knee Surg.*, 2003, **16**, 83–86.
- 14 H.-L. Ma, S.-C. Hung, S.-T. Wang, M.-C. Chang and T.-H. Chen, *Injury*, 2004, **35**, 1286–1292.
- 15 H. Robert, *Orthop. Traumatol.: Surg. Res.*, 2011, **97**, 418–429.
- 16 H. Kwon, W. E. Brown, C. A. Lee, D. Wang, N. Paschos, J. C. Hu and Kyriacos A. Athanasiou, *Nat. Rev. Rheumatol.*, 2019, **15**, 550–570.
- 17 F. J. O'Brien, *Mater. Today*, 2011, **14**, 88–95.
- 18 K. Pelttari, H. Lorenz, S. Boeuf, M. F. Templin, O. Bischel, K. Goetzke, H.-Y. Hsu, E. Steck and W. Richter, *Arthritis Rheum.*, 2008, **58**, 467–474.
- 19 E. B. Hunziker, K. Lippuner, M. J. B. Keel and N. Shintani, *Osteoarthritis Cartilage*, 2015, **23**, 334–350.
- 20 W. J. Choi, K. K. Park, B. S. Kim and J. W. Lee, *Am. J. Sports Med.*, 2009, **37**, 1974–1980.
- 21 K. S. Katti, *Colloids Surf., B*, 2004, **39**, 133–142.
- 22 L. E. Bayliss, D. Culliford, A. P. Monk, S. Glyn-Jones, D. Prieto-Alhambra, A. Judge, C. Cooper, A. J. Carr, N. K. Arden, D. J. Beard and A. J. Price, *Lancet*, 2017, **387**, 1424–1430.
- 23 D. I. Braghirrolli, D. Steffens and P. Pranke, *Drug Discovery Today*, 2014, **19**, 743–753.
- 24 N. Munir, A. McDonald and A. Callanan, *Bioprinting*, 2019, **16**, e00056.
- 25 M. Rafiei, E. Jooybar, M. J. Abdekhodaie and M. Alvi, *Mater. Sci. Eng., C*, 2020, **113**, 110913.
- 26 N. Toyokawa, H. Fujioka, T. Kokubu, I. Nagura, A. Inui, R. Sakata, M. Satake, H. Kaneko and M. Kurosaka, *Arthroscopy*, 2010, **26**, 375–383.
- 27 T. Nascimento da Silva, R. P. Gonçalves, C. L. Rocha, B. S. Archanjo, C. A. G. Barboza, M. B. R. Pierre, F. Reynaud and P. H. de Souza Picciani, *Mater. Sci. Eng., C*, 2019, **97**, 602–612.
- 28 J. A. Matthews, E. D. Boland, G. E. Wnek, D. G. Simpson and G. L. Bowlin, *J. Bioact. Compat. Polym.*, 2003, **18**, 125.
- 29 K. J. Shields, M. J. Beckman, G. L. Bowlin and J. S. Wayne, *Tissue Eng.*, 2004, **10**(9–10), 1510–1517.
- 30 J. Reignier and M. A. Huneault, *Polymer*, 2006, **47**, 4703–4717.
- 31 C.-J. Liao, C. F. Chen, J. H. Chen, S.-F. Chiang, Y.-J. Lin and K. Y. Chang, *J. Biomed. Mater. Res.*, 2002, **59**, 676–681.
- 32 D. C. Sin, X. Miao, G. Liu, F. Wei, G. Chadwick, C. Yan and T. Friis, *Mater. Sci. Eng., C*, 2010, **30**, 78–85.
- 33 N. Thadavirul, P. Pavasant and P. Supaphol, *J. Biomed. Mater. Res.*, 2014, **102**, 3379–3392.
- 34 V. Vishwanath, K. Pramanik and A. Biswas, *J. Biomater. Sci., Polym. Ed.*, 2016, **27**, 657–674.
- 35 Q. Zhang, H. Lu, N. Kawazoe and G. Chen, *Acta Biomater.*, 2014, **10**, 2005–2013.
- 36 W. Dai, N. Kawazoe, X. Lin, J. Dong and G. Chen, *Biomaterials*, 2010, **31**, 2141–2152.
- 37 S. A. Poursamar, A. N. Lehner, M. Azami, S. Ebrahimi-Barough, A. Samadikuchaksaraei and A. P. M. Antunes, *Mater. Sci. Eng., C*, 2016, **63**, 1–9.
- 38 W. L. Murphy, R. G. Dennis, J. L. Kileny and D. J. Mooney, *Tissue Eng.*, 2002, **8**, 43–52.
- 39 D. J. Mooney, D. F. Baldwin, N. P. Suh, J. P. Vacanti and R. Langer, *Biomaterials*, 1996, **17**, 1417–1422.
- 40 L. D. Harris, B.-S. Kim and D. J. Mooney, *J. Biomed. Mater. Res.*, 1998, **42**, 396–402.



41 A. Salerno, E. Di Maio, S. Iannace and P. A. Netti, *J. Porous Mater.*, 2012, **19**, 181–188.

42 I. Manavitehrani, T. Y. L. Le, S. Daly, Y. Wang, P. K. Maitz, A. Schindeler and F. Dehghani, *Mater. Sci. Eng., C*, 2019, **96**, 824–830.

43 C. M. Murphy, M. G. Haugh and F. J. O'Brien, *Biomaterials*, 2010, **31**, 461–466.

44 C. M. Murphy, A. Matsiko, M. G. Haugh, J. P. Gleeson and F. J. O'Brien, *J. Mech. Behav. Biomed. Mater.*, 2012, **11**, 53–62.

45 F. J. O'Brien, B. A. Harley, I. V. Yannas and L. J. Gibson, *Biomaterials*, 2005, **26**, 433–441.

46 T. J. Levingstone, A. Matsiko, G. R. Dickson, F. J. O'Brien and J. P. Gleeson, *Acta Biomater.*, 2014, **10**, 1996–2004.

47 C. M. Tierney, M. G. Haugh, J. Liedl, F. Mulcahy, B. Hayes and F. J. O'Brien, *J. Mech. Behav. Biomed. Mater.*, 2009, **2**, 202–209.

48 L. Moroni, J. A. Burdick, C. B. Highley, S. J. Lee, Y. Morimoto and S. Takeuchi, *Nat. Rev. Mater.*, 2018, **3**, 21–37.

49 R. M. Raftery, D. P. Walsh, L. B. Ferreras, I. M. Castaño, G. Chen, M. Lemoine, G. Osman, K. M. Shakesheff, J. E. Dixon and F. J. O'Brien, *Biomaterials*, 2019, **216**, 119277.

50 T. Gonzalez-Fernandez, S. Rathan, C. Hobbs, P. Pitacco, F. E. Freeman, G. M. Cunniffe, N. J. Dunne, H. O. McCarthy, V. Nicolosi, F. J. O'Brien and D. J. Kelly, *J. Controlled Release*, 2019, **301**, 13–27.

51 X. Hu, Y. Man, W. Li, L. Li, J. Xu, R. Parungao, Y. Wang, S. Zheng, Y. Nie, T. Liu and K. Song, *Polymers*, 2019, **11**, 10.

52 A. C. Daly, F. E. Freeman, T. Gonzalez-Fernandez, S. E. Critchley, J. Nulty and D. J. Kelly, *Adv. Healthcare Mater.*, 2017, **6**, 22.

53 M. E. Prendergast and J. A. Burdick, *Adv. Mater.*, 2020, **32**, 13.

54 J. Malda, J. Visser, F. P. Melchels, T. Jüngst, W. E. Hennink, W. J. A. Dhert, J. Groll and D. W. Hutmacher, *Adv. Mater.*, 2013, **25**, 5011–5028.

55 M. Singh, H. M. Haverinen, P. Dhagat and G. E. Jabbour, *Adv. Mater.*, 2010, **22**, 673–685.

56 A. Negro, T. Cherbuin and M. P. Lutolf, *Sci. Rep.*, 2018, **8**, 17099.

57 Dassault Systèmes, 3D Printing – Additive, (accessed 01/04/2020).

58 L. Koch, M. Gruene, C. Unger and B. Chichkov, *Curr. Pharm. Biotechnol.*, 2013, **14**, 91–97.

59 N. Paxton, W. Smolan, T. Böck, F. P. Melchels, J. Groll and T. Jüngst, *Biofabrication*, 2017, **9**, 4.

60 J. Groll, J. A. Burdick, D.-W. Cho, B. Derby, M. Gelinksy, S. C. Heilshorn, T. Jüngst, J. Malda, V. A. Mironov, K. Nakayama, A. Ovsianikov, W. Sun, S. Takeuchi, J. J. Yoo and T. B. F. Woodfield, *Biofabrication*, 2019, **11**, 1.

61 A. M. Bhosale and J. B. Richardson, *Br. Med. Bull.*, 2008, **87**, 77–95.

62 A. Matsiko, T. J. Levingstone and F. J. O'Brien, *Materials*, 2013, **6**, 637–668.

63 A. R. Armiento, M. J. Stoddart, M. Alini and D. Eglin, *Acta Biomater.*, 2018, **65**, 1–20.

64 A. J. S. Fox, A. Bedi and S. A. Rodeo, *Sports Health*, 2009, **1**, 461–468.

65 K. Gelse, E. Poschl and T. Aigner, *Adv. Drug Delivery Rev.*, 2003, **55**, 1531–1546.

66 K. E. Kadler, A. Hill and E. G. Carty-Laird, *Curr. Opin. Cell Biol.*, 2008, **20**, 495–501.

67 J. Casale and J. S. Crane, *Biochemistry, Glycosaminoglycans*, StatPearls Publishing LLC, 2021, <https://www.ncbi.nlm.nih.gov/books/NBK544295/> [Accessed on 18/05/21].

68 P. J. Roughley and J. S. Mort, *J. Exp. Orthop.*, 2014, **1**, 8.

69 A. R. Poole, T. Kojima, T. Yasuda, F. Mwale, M. Kobayashi and S. Laverty, *Clin. Orthop. Relat. Res.*, 2001, **391S**, S26–S33.

70 H. Akkiraju and A. Nohe, *J. Dev. Biol.*, 2015, **3**, 177–192.

71 J. W. Alford and Brian J. Cole, *Am. J. Sports Med.*, 2005, **33**(2), 295–306.

72 J. A. Buckwalter and H. J. Mankin, *Instr. Course Lect.*, 1998, **47**, 477–486.

73 D. Baksh, L. Song and R. S. Tuan, *J. Cell. Mol. Med.*, 2004, **8**, 301–316.

74 M. Dominici, K. Le Blanc, I. Mueller, I. Slaper-Cortenbach, F. C. Marini, D. S. Krause, R. J. Deans, A. Keating, D. J. Prockop and E. M. Horwitz, *Cryotherapy*, 2006, **8**, 315–317.

75 C. N. D. Coelho and R. A. Kosher, *Dev. Biol.*, 1991, **144**, 47–53.

76 M. B. Goldring, K. Tsuchimochi and K. Ijiri, *J. Cell. Biochem.*, 2006, **97**, 33–44.

77 L. Shum and G. Nuckolls, *Arthritis Res.*, 2002, **4**, 94–106.

78 J. D. Green, V. Tollemar, M. Dougherty, Z. Yan, L. Yin, J. Ye, Z. Collier, M. K. Mohammed, R. C. Haydon, H. H. Luu, R. Kang, M. J. Lee, S. H. Ho, T.-C. He, L. L. Shi and A. Athiviraham, *Genes Dis.*, 2015, **2**, 307–327.

79 L. Yang, K. Y. Tsang, H. C. Tang, D. Chan and K. S. E. Cheah, *Proc. Natl. Acad. Sci. U. S. A.*, 2014, **111**, 12097–12102.

80 M. Wang, E. R. Sampson, H. Jin, J. Li, Q. H. Ke, H.-J. Im and D. Chen, *Arthritis Res. Ther.*, 2013, **15**, 1.

81 U. Sharma, D. Pal and R. Prasad, *Indian J. Clin. Biochem.*, 2014, **29**, 269–278.

82 R. Dreier, *Arthritis Res. Ther.*, 2010, **12**, 216.

83 M. Ding, Y. Lu, S. Abbassi, F. Li, X. Li, Y. Song, V. Geoffroy, H.-J. Im and Q. Zheng, *J. Cell. Physiol.*, 2012, **227**, 3446–3456.

84 Y.-Q. Yang, Y.-Y. Tan, R. Wong, A. Wenden, L.-K. Zhang and A. B. M. Rabie, *Int. J. Oral Sci.*, 2012, **4**, 64–68.

85 E. M. Ahmed, *J. Adv. Res.*, 2015, **6**, 105–121.

86 S. Uman, A. P. Dhand and J. A. Burdick, *J. Appl. Polym. Sci.*, 2019, **137**, 25.

87 M. Guvendiren, H. D. Lu and J. A. Burdick, *Soft Matter*, 2012, **2**, 260–272.



88 F. L. C. Morgan, L. Moroni and M. B. Baker, *Adv. Healthcare Mater.*, 2020, **9**, 15.

89 S. Ji and M. Guvendiren, *Front. Bioeng. Biotechnol.*, 2017, **5**, 23.

90 A. Panwar and L. P. Tan, *Molecules*, 2016, **21**, 685.

91 E. O. Osidak, V. I. Kozhukhov, M. S. Osidak and S. P. Domogatsky, *Int. J. Bioprint.*, 2020, **6**, 270.

92 M. Hospodiu, M. Dey, D. Sosnoski and I. T. Ozbolat, *Biotechnol. Adv.*, 2017, **35**, 217–239.

93 V. L. Cross, Y. Zheng, N. W. Choi, S. S. Verbridge, B. A. Sutermaster, L. J. Bonassar, C. Fischback and A. D. Stroock, *Biomaterials*, 2010, **31**, 8596–8607.

94 S. Rhee, J. L. Puetzer, B. N. Mason, C. A. Reinhart-King and L. J. Bonassar, *ACS Biomater. Sci. Eng.*, 2016, **2**(10), 1800–1805.

95 Advanced BioMatrix, Lifeink 200 – Neutralized Type I Collagen Bioink, 3.5 mg mL<sup>-1</sup> (accessed 27/05/21).

96 Imtek Ltd, Viscoll Collagen Solution – Pig collagen type I, sterile solution (accessed 27/05/21).

97 E. O. Osidak, P. A. Karalkin, M. S. Osidak, V. A. Parfenov, D. E. Sivogrivov, F. D. A. S. Pereira, A. A. Gryadunova, E. V. Koudan, Y. D. Khesuani, V. A. Kasyanov, S. I. Belousov, S. V. Krasheninnikov, T. E. Grigoriev, S. N. Chvalun, E. A. Bulanova, V. A. Mironov and S. P. Domogatsky, *J. Mater. Sci.: Mater. Med.*, 2019, **30**(31).

98 J. M. Lee, S. K. Q. Suen, W. L. Ng, W. C. Ma and W. Y. Yeong, *Macromol. Biosci.*, 2021, **21**, 1.

99 Y. W. Koo, E.-J. Choi, J. Y. Lee, H.-J. Kim, G. H. Kim and S. H. Do, *J. Ind. Eng. Chem.*, 2018, **66**, 343–355.

100 G. Montalbano, G. Borciani, G. Cerqueni, C. Licini, F. Banche-Nicot, D. Janner, S. Sola, S. Fiorilli, M. Mattioli-Belmonte, G. Ciapetti and C. Vitale-Brovarone, *Nanomaterials*, 2020, **10**, 1681.

101 Y. B. Kim, H. Lee and G. H. Kim, *ACS Appl. Mater. Interfaces*, 2016, **8**, 32230–32240.

102 T.-U. Nguyen, K. E. Watkins and V. Kishore, *J. Biomed. Mater. Res., Part A*, 2019, **107**, 1541–1550.

103 K. E. Drzewiecki, A. S. Parmar, I. D. Gaudet, J. R. Branch, D. H. Pike, V. Nanda and D. I. Shreiber, *Langmuir*, 2014, **30**, 11204–11211.

104 N. S. Kajave, T. Schmitt, T.-U. Nguyen and V. Kishore, *Mater. Sci. Eng., C*, 2020, **107**, 110290.

105 N. S. Kajave, T. Schmitt, T.-U. Nguyen, A. K. Gaharwar and V. Kishore, *Biomed. Mater.*, 2021, **16**, 3.

106 I. D. Gaudet and D. I. Shreiber, *Biointerphases*, 2012, **7**, 25.

107 K. Guo, H. Wang, S. Li, H. Zhang, S. Li, H. Zhu, Z. Yang, L. Zhang, P. Chang and X. Zheng, *ACS Appl. Mater. Interfaces*, 2021, **13**, 7037–7050.

108 T. J. Hinton, Q. Jallerat, R. N. Palchesko, J. H. Park, M. S. Grodzicki, H.-J. Shue, M. H. Ramadan, A. R. Hudson and A. W. Feinberg, *Sci. Adv.*, 2015, **1**, e1500758.

109 D. J. Shirwarski, A. R. Hudson, J. W. Tashman and A. W. Feinberg, *APL Bioeng.*, 2021, **5**, 010904.

110 A. Lee, A. R. Hudson, D. J. Shirwarski, J. W. Tashman, T. J. Hinton, S. Yerneni, J. M. Bliley, P. G. Campbell and A. W. Feinberg, *Science*, 2019, **365**, 482–487.

111 T. Sousa, N. S. Kajave, P. Dong, L. Gu, S. Florkzyk and V. Kishore, *3D Printing and Additive Manufacturing*, 2021, Ahead of print.

112 M. Santoro, A. M. Tatara and A. G. Mikos, *J. Controlled Release*, 2014, **190**, 210–218.

113 M. B. Łabowska, K. Cierluk, A. M. Jankowska, J. Kulbacka, J. Detyna and I. Michalak, *Materials*, 2021, **14**, 858.

114 W. Schuurman, P. A. Levett, M. W. Pot, P. R. van Weeren, W. J. A. Dhert, D. W. Hutmacher, F. P. W. Melchels, T. J. Klein and J. Malda, *Macromol. Biosci.*, 2013, **13**, 551–561.

115 Y. P. Singh, A. Bandyopadhyay and B. B. Mandal, *ACS Appl. Mater. Interfaces*, 2019, **11**, 33684–33696.

116 S. Chawla, A. Kumar, P. Admane, A. Bandyopadhyay and S. Ghosha, *Bioprinting*, 2017, **7**, 1–13.

117 S. Chawla, G. Desando, E. Gabusi, A. Sharma, D. Trucco, J. Chakraborty, C. Manferdini, M. Petretta, G. Lisignoli and S. Ghosh, *J. Mater. Res.*, 2021, **36**, 4051–4067.

118 S. Schwarza, S. Kuthab, T. Distler, C. Gögele, K. Stölzel, R. Detsch, A. R. Boccaccini and G. Schulze-Tanzil, *Mater. Sci. Eng., C*, 2020, **116**, 111189.

119 J. Visser, B. Peters, T. J. Burger, J. Boomstra, W. J. A. Dhert, F. P. W. Melchels and J. Malda, *Biofabrication*, 2013, **5**, 3.

120 Q. Gao, X. Niu, L. Shao, L. Zhou, Z. Lin, A. Sun, J. Fu, Z. Chen, J. Hu and Y. Liu, *Biofabrication*, 2019, **11**, 3.

121 J. Liu, L. Li, H. Suo, M. Yan, J. Yin and J. Fu, *Mater. Des.*, 2019, **171**, 107708.

122 V. H. M. Mouser, R. Levato, A. Mensinga, W. J. A. Dhert, D. Gawlitta and J. Malda, *Connect. Tissue Res.*, 2018, **61**, 137–151.

123 J. S. Lee, H. S. Park, H. Jung, H. Lee, H. Hong, Y. J. Lee, Y. J. Suh, O. J. Lee, S. H. Kim and C. H. Park, *Addit. Manuf.*, 2020, **33**, 101136.

124 R. Schipani, S. Scheurer, R. Florentin, S. E. Critchley and D. J. Kelly, *Biofabrication*, 2020, **12**, 3.

125 F. Gao, Z. Xu, Q. Liang, H. Li, L. Peng, M. Wu, X. Zhao, X. Cui, C. Ruan and W. Liu, *Adv. Sci.*, 2019, **6**, 15.

126 S. Duchi, C. Onofrillo, C. D. O'Connell, R. Blanchard, C. Augustine, A. F. Quigley, R. M. I. Kapsa, P. Pivonka, G. G. Wallace, C. Di Bella and P. F. M. Choong, *Sci. Rep.*, 2017, **7**, 5387.

127 K. S. Lim, F. Abinzano, P. N. Bernal, A. A. Sanchez, P. Atienza-Roca, I. A. Otto, Q. C. Peiffer, M. Matsusaki, T. B. F. Woodfield, J. Malda and R. Levato, *Adv. Healthcare Mater.*, 2020, **9**, 1901792.

128 J. A. Burdick and G. D. Prestwich, *Adv. Mater.*, 2011, **23**, H41–H56.

129 E. D. Bonnevie, D. Galessio, C. Secchieri, I. Cohen and L. J. Bonassar, *PLoS One*, 2015, **10**, e0143415.

130 C. B. Knudson, *Birth Defects Res., Part C*, 2003, **69**, 174–196.

131 C. Chung and J. A. Burdick, *Tissue Eng., Part A*, 2008, **15**, 2.

132 W. S. Toh, T. C. Lim, M. Kurisawa and M. Spector, *Biomaterials*, 2012, **33**, 3835–3845.



133 I. L. Kim, S. Khetan, B. M. Baker, C. S. Chen and J. A. Burdick, *Biomaterials*, 2013, **34**, 5571–5580.

134 I. E. Erickson, A. H. Huang, S. Sengupta, S. Kestle, J. A. Burdick and R. L. Mauck, *Osteoarthritis Cartilage*, 2009, **17**, 1639–1648.

135 A. A. Hegewald, J. Ringe, J. Bartel, I. Krüger, M. Notter, D. Barnewitz, C. Kaps and M. Sittinger, *Tissue Cell*, 2004, **36**, 431–438.

136 R. B. Jakobsen, A. Shahdadfar, F. P. Reinholt and J. E. Brinchmann, *Knee Surg. Sports Traumatol. Arthrosc.*, 2010, **18**, 1407–1416.

137 A. Matsiko, T. J. Levingstone, F. J. O'Brien and J. P. Gleeson, *J. Mech. Behav. Biomed. Mater.*, 2012, **11**, 41–52.

138 I. L. Kim, R. L. Mauck and J. A. Burdick, *Biomaterials*, 2011, **32**, 8771–8782.

139 L. A. Solchaga, J. E. Dennis, V. M. Goldberg and A. I. Caplan, *J. Orthop. Res.*, 1999, **17**, 205–213.

140 Y. Jin, R. H. Koh, S.-H. Kim, K. M. Kim, G. K. Park and N. S. Hwang, *Mater. Sci. Eng., C*, 2020, **115**, 111096.

141 L. Valot, J. Martinez, A. Mehdi and G. Subra, *Chem. Soc. Rev.*, 2019, **48**, 3999–4340.

142 D. Petta, U. D'Amora, L. Ambrosio, D. W. Grijpma, D. Eglin and M. D'Este, *Biofabrication*, 2020, **12**, 3.

143 C. Antich, J. de Vicente, G. Jiménez, C. Chocarro, E. Carrillo, E. Montañez, P. Gálvez-Martín and J. A. Marchal, *Acta Biomater.*, 2020, **106**, 114–123.

144 M. Lafuente-Merchan, S. Ruiz-Alonso, A. Espina-Noguera, P. Galvez-Martin, E. López-Ruiz, J. A. Marchal, M. L. López-Donaire, A. Zabala, J. Ciriza, L. Saenz-del-Burgo and J. L. Pedraz, *Mater. Sci. Eng., C*, 2021, **126**, 112160.

145 S. J. Lee, J. M. Seok, J. H. Lee, J. Lee, W. D. Kim and S. A. Park, *Polymers*, 2021, **13**, 794.

146 C. C. Piras and D. K. Smith, *J. Mater. Chem. B*, 2020, **8**, 8171–8188.

147 I. Noh, N. Kim, H. N. Tran, J. Lee and C. Lee, *Biomater. Res.*, 2019, **23**, 3.

148 B. Wang, P. J. Díaz-Payno, D. C. Browne, F. E. Freeman, J. Nulty, R. Burdis and D. J. Kelly, *Acta Biomater.*, 2021, **128**, 130–142.

149 K. Y. Lee and D. J. Mooney, *Prog. Polym. Sci.*, 2012, **37**, 106–126.

150 C. B. Highley, G. D. Prestwich and J. A. Burdick, *Curr. Opin. Biotechnol.*, 2016, **40**, 35–40.

151 B. S. Spearman, N. K. Agrawal, A. Rubiano, C. S. Simmons, S. Mobini and C. E. Schmidt, *J. Biomed. Mater. Res.*, 2020, **108A**, 279–291.

152 M. T. Poldervaart, B. Goversen, M. de Ruijter, A. Abbadessa, F. P. W. Melchels, F. C. Öner, W. J. A. Dhert, T. Vermonden and J. Alblas, *PLoS One*, 2017, **12**, 6.

153 J. A. Burdick, C. Chung, X. Jia, M. A. Randolph and R. Langer, *Biomacromolecules*, 2005, **6**, 386–391.

154 M. Y. Kwon, C. Wang, J. H. Galarraga, E. Puré, L. Han and J. A. Burdick, *Biomaterials*, 2019, **222**, 119451.

155 Q. Mei, J. Rao, H. P. Bei, Y. Liu and X. Zhao, *Int. J. Bioprint.*, 2021, **7**, 367.

156 M. Kesti, M. Müller, J. Becher, M. Schnabelrauch, M. D'Este, D. Eglin and M. Zenobi-Wong, *Acta Biomater.*, 2015, **11**, 162–172.

157 J. H. Galarraga, M. Y. Kwon and J. A. Burdick, *Sci. Rep.*, 2019, **9**, 19987.

158 S. Stichler, T. Böck, N. Paxton, S. Bertlein, R. Levato, V. Schill, W. Smolan, J. Malda, J. Teßmar, T. Blunk and J. Groll, *Biofabrication*, 2017, **9**, 4.

159 J. Hauptstein, T. Böck, M. Bartolf-Kopp, L. Forster, P. Stahlhut, A. Nadernezhad, G. Blahetek, A. Zernecke-Madsen, R. Detsch, T. Jüngst, J. Groll, J. Teßmar and T. Blunk, *Adv. Healthcare Mater.*, 2020, **9**(15).

160 D. Nguyen, D. A. Hägg, A. Forsman, J. Ekholm, P. Nimkingratana, C. Brantsing, T. Kalogeropoulos, S. Zaunz, S. Concaro, M. Brittberg, A. Lindahl, P. Gatenholm, A. Enejder and S. Simonsson, *Sci. Rep.*, 2017, **7**, 658.

161 A. K.-X. Lee, Y.-H. Lin, C.-H. Tsai, W.-T. Chang, T.-L. Lin and M.-Y. Shie, *Biomedicines*, 2021, **9**(7), 714.

162 S. Nedunchezian, P. Banerjee, C.-Y. Lee, S.-S. Lee, C.-W. Lin, C.-W. Wu, S.-C. Wu, J.-K. Chang and C.-K. Wang, *Mater. Sci. Eng., C*, 2021, **124**, 112072.

163 P. L. Thi, J. Y. Son, Y. Lee, S. B. Ryu, K. M. Park and K. D. Park, *Macromol. Res.*, 2020, **28**, 400–406.

164 K. J. Wolf and S. Kumar, *ACS Biomater. Sci. Eng.*, 2019, **5**, 3753–3765.

165 J.-T. Kim, D. Y. Lee, Y.-H. Kim, I.-K. Lee and Y.-S. Song, *J. Sens. Sci. Technol.*, 2012, **21**, 256–262.

166 C. Kiani, L. Chen, Y. J. Wu, A. J. Yee and B. B. Yang, *Cell Res.*, 2002, **12**, 19–32.

167 H. Watanabe, Y. Yamada and K. Kimata, *J. Biochem.*, 1998, **124**, 687–693.

168 J. J. Lim and J. S. Temenoff, *Biomaterials*, 2013, **34**, 5007–5018.

169 J. Radhakrishnan, A. Subramanian, U. M. Krishnan and S. Sethuraman, *Biomacromolecules*, 2017, **18**, 1–26.

170 S. Varghese, N. S. Hwang, A. C. Canver, P. Theprungsirikul, D. W. Lin and J. Elisseeff, *Matrix Biol.*, 2008, **27**, 12–21.

171 C. S. Moura, J. C. Silva, S. Faria, P. R. Fernandes, C. L. da Silva, J. M. S. Cabral, R. Linhardt, P. J. Bárto and F. C. Ferreira, *J. Biosci. Bioeng.*, 2020, **129**, 756–764.

172 E. A. Aisenbrey and S. J. Bryant, *Biomaterials*, 2019, **190–191**, 51–62.

173 T. Li, X. Song, C. Weng, X. Wang, L. Sun, X. Gong, L. Yang and C. Chen, *Appl. Mater. Today*, 2018, **10**, 173–183.

174 C. Tang, B. D. Holt, Z. M. Wright, A. M. Arnold, A. C. Moy and S. A. Sydlik, *J. Mater. Chem. B*, 2019, **7**, 2442–2453.

175 X. Li, Q. Xu, M. Johnson, X. Wang, J. Lyu, Y. Li, S. McMahon, U. Greiser, S. A and W. Wang, *Biomater. Sci.*, 2021, **9**, 4139–4148.

176 S. Lee, J. Choi, J. Youn, Y. Lee, W. Kim, S. Choe, J. Song, R. L. Reis and G. Khang, *Biomolecules*, 2021, **11**, 8.



177 M. Liu, X. Zeng, C. Ma, H. Yi, Z. Ali, X. Mou, S. Li, Y. Deng and N. He, *Bone Res.*, 2017, **5**, 17014.

178 P. A. Levett, F. P. W. Melchels, K. Schrobback, D. W. Hutmacher, J. Malda and T. J. Klein, *Acta Biomater.*, 2014, **10**, 214–223.

179 A. Khanlari, M. S. Detamore and S. H. Gehrke, *Macromolecules*, 2013, **46**, 9609–9617.

180 X. Liu, S. Liu, R. Yang, P. Wang, W. Zhang, X. Tan, Y. Ren and B. Chi, *Carbohydr. Polym.*, 2021, **270**, 118330.

181 M. Costantini, J. Idaszek, K. Szöke, J. Jaroszewicz, M. Dentini, A. Barbetta, J. E. Brinchmann and W. Święszkowski, *Biofabrication*, 2016, **8**(3).

182 A. Abbadessa, V. H. M. Mouser, M. M. Blokzijl, D. Gawlitta, W. J. A. Dhert, W. E. Hennink, J. Malda and T. Vermonden, *Biomacromolecules*, 2016, **17**, 2137–2147.

183 A. Scalzone, M. A. Bonifacio, S. Cometa, F. Cucinotta, E. De Giglio, A. M. Ferreira and P. Gentile, *Front. Bioeng. Biotechnol.*, 2020, **8**, 712.

184 J. Shin, E. H. Kang, S. Choi, E. J. Jeon, J. H. Cho, D. Kang, H. Lee, I. S. Yun and S.-W. Cho, *ACS Biomater. Sci. Eng.*, 2021, **7**, 4230–4243.

185 A. Abbadessa, M. M. Blokzijl, V. H. M. Mouser, P. Marica, J. Malda, W. E. Hennink and T. Vermonden, *Carbohydr. Polym.*, 2016, **149**, 163–174.

186 A. J. Vernengo, S. Grad, D. Eglin, M. Alini and Z. Li, *Adv. Funct. Mater.*, 2020, **30**, 1909044.

187 T. W. Gilbert, T. L. Sellaro and S. F. Badylak, *Biomaterials*, 2006, **27**, 3675–3683.

188 P. M. Crapo, T. W. Gilbert and S. F. Badylak, *Biomaterials*, 2011, **32**, 3233–3243.

189 F. Pati, J. Jang, D.-H. Ha, S. W. Kim, J.-W. Rhie, J.-H. Shim, D.-H. Kim and D.-W. Cho, *Nat. Commun.*, 2014, **5**, 3935.

190 D. O. Visscher, H. Lee, P. P. M. van Zuijlen, M. N. Helder, A. Atala, J. J. Yoo and S. J. Lee, *Acta Biomater.*, 2021, **121**, 193–203.

191 C. S. Jung, B. K. Kim, J. Lee, B.-H. Min and S.-H. Park, *Tissue Eng. Regener. Med.*, 2018, **15**, 155–162.

192 S. Rathan, L. Dejob, R. Schipani, B. Haffner, M. E. Möbius and D. J. Kelly, *Adv. Healthcare Mater.*, 2019, **8**, 7.

193 X. Zhang, Y. Liu, C. Luo, C. Zhai, Z. Li, Y. Zhang, T. Yuan, S. Dong, J. Zhang and W. Fan, *Mater. Sci. Eng., C*, 2021, **118**, 111388.

194 W. Chen, Y. Xu, Y. Li, L. Jia, X. Mo, G. Jiang and G. Zhou, *Chem. Eng. J.*, 2020, **382**, 122986.

195 A. Abaci and M. Guvendiren, *Adv. Healthcare Mater.*, 2020, **9**, 2000734.

196 D. O. Freytes, J. Martin, S. S. Velankar, A. S. Lee and S. F. Badylak, *Biomaterials*, 2008, **29**, 1630–1637.

197 M. Setayeshmehr, S. Hafeez, C. van Blitterswijk, L. Moroni, C. Mota and M. B. Baker, *Int. J. Mol. Sci.*, 2021, **22**, 8.

198 M. S. Silverstein, *Polymer*, 2020, **207**, 122929.

199 S. L. Vega, M. Y. Kwon and J. A. Burdick, *Eur. Cells Mater.*, 2017, **30**, 59–75.

200 A. P. Dhand, J. H. Galarraga and J. A. Burdick, *Trends Biotechnol.*, 2021, **39**, 519–538.

201 D. Chimene, R. Kaunas and A. K. Gaharwar, *Adv. Mater.*, 2020, **32**, 1.

202 I.-C. Liao, F. T. Moutos, B. T. Estes, X. Zhao and F. Guilak, *Adv. Funct. Mater.*, 2013, **23**, 5833–5839.

203 W. Li, D. Wu, D. Hu, S. Zhu, C. Pan, Y. Jiao, L. Li, B. Luo, C. Zhou and L. Lu, *Mater. Sci. Eng., C*, 2020, **107**, 110333.

204 O. Chaudhuri, J. Cooper-White, P. A. Janmey, D. J. Mooney and V. B. Shenoy, *Nature*, 2020, **584**, 535–546.

205 J. S. Park, J. S. Chu, A. D. Tsou, R. Diop, Z. Tang, A. Wang and S. Li, *Biomaterials*, 2011, **32**, 3921–3930.

206 A. S. Mao, J.-W. Shin and D. J. Mooney, *Biomaterials*, 2016, **98**, 184–191.

207 A. J. Steward and D. J. Kelly, *J. Anat.*, 2015, **227**, 717–731.

208 H.-p. Lee, L. Gu, D. J. Mooney, M. E. Levenston and O. Chaudhuri, *Nat. Mater.*, 2017, **16**, 1243–1251.

209 D. Wu, Y. Yu, J. Tan, L. Huang, B. Luo, L. Lu and C. Zhou, *Mater. Des.*, 2018, **160**, 486–495.

210 T. Ni, M. Liu, Y. Zhang, Y. Cao and R. Pei, *Bioconjugate Chem.*, 2020, **31**, 1938–1947.

211 X. Yang, Z. Lu, H. Wu, W. Li, Li Zheng and J. Zhao, *Mater. Sci. Eng., C*, 2018, **83**, 195–201.

212 N. Diamantides, C. Dugopolski, E. Blahut, S. Kennedy and L. J. Bonassar, *Biofabrication*, 2019, **11**, 045016.

213 A. Schwab, C. Hélary, R. G. Richards, M. Alini, D. Eglin and M. D'Este, *Mater. Today Bio*, 2020, **7**, 100058.

214 Y. Zhou, R. Qin, T. Chen, K. Zhang and J. Gui, *Mater. Des.*, 2021, **203**, 109621.

215 C. Henrionnet, L. Pourchet, P. Neybecker, O. Messaoudi, P. Gillet, D. Loeuille, D. Mainard, C. Marquette and A. Pinzano, *Stem Cells Int.*, 2020, **2020**, 2487072.

216 I. Pepelanova, K. Kruppa, T. Schepers and A. Lavrentieva, *Bioengineering*, 2018, **5**, 55.

217 M. Lafuente-Merchan, S. Ruiz-Alonso, A. Zabala, P. Gálvez-Martín, J. A. Marchal, B. Vázquez-Lasa, I. Gallego, L. Saenz-del-Burgo and J. L. Pedraz, *Macromol. Biosci.*, 2022, **22**(3), 2100435.

218 R. Contentin, M. Demoor, M. Concari, M. Desancé, F. Audigé, T. Branly and P. Galéra, *Stem Cell Rev. Rep.*, 2020, **16**(1), 126–143.

219 J. A. Semba, A. A. Mieloch and J. D. Rybk, *Bioprinting*, 2020, **18**, e00070.

220 O. Jeon, Y. B. Lee, T. J. Hinton, A. W. Feinberg and E. Alsberg, *Mater. Today Chem.*, 2019, **12**, 61–70.

221 C. Luo, R. Xie, J. Zhang, Y. Liu, Z. Li, Y. Zhang, X. Zhang, T. Yuan, Y. Chen and W. Fan, *Tissue Eng., Part C*, 2020, **26**, 306–316.

222 J. Yin, M. Yan, Y. Wang, J. Fu and H. Suo, *ACS Appl. Mater. Interfaces*, 2018, **10**, 6849–6857.

223 Y. Sun, Y. You, W. Jiang, B. Wang, Q. Wu and K. Dai, *Sci. Adv.*, 2020, **6**(37).

224 Y. Sun, Y. You, W. Jiang, Z. Zhai and K. Dai, *Theranostics*, 2019, **9**(23), 6949–6961.

225 R. Levato, W. R. Webb, I. A. Otto, A. Mensinga, Y. Zhang, M. van Rijen, R. van Weeren, I. M. Khan and J. Malda, *Acta Biomater.*, 2017, **1**(61), 41–53.



226 P. Diloksumpan, M. de Ruijter, M. Castilho, U. Gbureck, T. Vermonden, P. R. van Weeren, J. Malda and R. Levato, *Biofabrication*, 2020, **12**(2).

227 E. Vinod, R. Parameswaran, B. Ramasamy and U. Kachroo, *Cartilage*, 2021, **12**(2\_suppl), 34S–52S.

228 I. M. Khan, J. C. Bishop, S. Gilbert and C. W. Archer, *Osteoarthritis Cartilage*, 2009, **17**, 518–528.

229 C. T. Jayasuriya and Q. Chen, *Connect. Tissue Res.*, 2015, **56**(4), 265–271.

230 H. Chen, F. Fei, X. Li, Z. Nie, D. Zhou, L. Liu, J. Zhang, H. Zhang, Z. Fei and T. Xu, *Bioact. Mater.*, 2021, **6**(10), 3580–3595.

231 J. M. Baena, G. Jiménez, E. López-Ruiz, C. Antich, C. Grifán-Lisón, M. Perán, P. Gálvez-Martín and J. A. Marchal, *Exp. Biol. Med.*, 2019, **244**, 1.

232 J. Idaszek, M. Costantini, T. A. Karlsen, J. Jaroszewicz, C. Colosi, S. Testa, E. Fornetti, S. Bernardini, M. Seta, K. Kasarełło, R. Wrzesień, S. Cannata, A. Barbetta, C. Gargioli, J. E. Brinchman and W. Świeżkowski, *Biofabrication*, 2019, **11**, 4.

233 K. M. Hubka, R. L. Dahlin, V. V. Meretoja, F. K. Kasper and A. G. Mikos, *Tissue Eng., Part B*, 2014, **20**(6), 641–654.

234 K. Pelttari, H. Lorenz, S. Boeuf, M. F. Templin, O. Bischel, K. Goetzke, H.-Y. Hsu, E. Steck and W. Richter, *Arthritis Rheum.*, 2008, **58**(2), 467–474.

235 E. B. Hunziker, T. M. Quinn and H.-J. Häuselmann, *Osteoarthritis Cartilage*, 2002, **10**, 564–572.

236 X. Ren, F. Wang, C. Chen, X. Gong, L. Yin and L. Yang, *BMC Musculoskeletal Disord.*, 2016, **17**, 301.

237 L. Zhou, G. J. V. M. van Osch, J. Malda, M. J. Stoddart, Y. Lai, R. G. Richards, K. K.-w. Ho and L. Qin, *Adv. Healthcare Mater.*, 2020, **9**(23).

238 R. M. Raftery, I. M. Castaño, S. Sperger, G. Chen, B. Cavanagh, G. A. Feichtinger, H. Redl, A. Hacobian and F. J. O'Brien, *J. Controlled Release*, 2018, **283**, 20–31.

239 C. M. Curtin, E. G. Tierney, K. McSorley, S.-A. Cryan, G. P. Duffy and F. J. O'Brien, *Adv. Healthcare Mater.*, 2015, **4**, 223–227.

240 C. M. Curtin, G. M. Cunniffe, F. G. Lyons, K. Bessho, G. R. Dickson, G. P. Duffy and F. J. O'Brien, *Adv. Mater.*, 2012, **24**, 749–754.

241 R. M. Raftery, I. M. Castaño, G. Chen, B. Cavanagh, B. Quinn, C. M. Curtin, S.-A. Cryan and F. J. O'Brien, *Biomaterials*, 2017, **149**, 116–127.

242 Z. Yu, Y. Li, Y. Wang, Y. Chen, M. Wu, Z. Wang, M. Song, F. Lu, X. Lu and Z. Dong, *Biosci. Rep.*, 2019, **39**.

243 J. R. García, A. Y. Clark and A. J. García, *J. Biomed. Mater. Res., Part A*, 2016, **104**, 889–900.

244 A. I. Caplan and D. Correa, *J. Orthop. Res.*, 2011, **29**, 1795–1803.

245 R. M. Raftery, A. G. Gonzalez Vazquez, G. Chen and F. J. O'Brien, *Adv. Healthcare Mater.*, 2020, **9**, 1901827.

246 N. van Gastel, S. Stegen, G. Eelen, S. Schoors, A. Carlier, V. W. Daniëls, N. Baryawno, D. Przybylski, M. Depypere, P.-J. Stiers, D. Lambrechts, R. Van Looveren, S. Torrekens, A. Sharda, P. Agostinis, D. Lambrechts, F. Maes, J. V. Swinnen, L. Geris, H. Van Oosterwyck, B. Thienpont, P. Carmeliet, D. T. Scadden and G. Carmeliet, *Nature*, 2020, **579**, 111–117.

247 I. Sekiya, J. T. Vuoristo, B. L. Larson and D. J. Prockop, *Proc. Natl. Acad. Sci. U. S. A.*, 2002, **99**, 4397–4402.

248 B. Johnstone, T. M. Hering, A. I. Caplan, V. M. Goldberg and J. U. Yoo, *Exp. Cell Res.*, 1998, **238**, 265–272.

249 F. Barry, R. E. Boynton, B. Liu and J. M. Murphy, *Exp. Cell Res.*, 2001, **268**, 189–200.

250 M. E. Joyce, A. B. Roberts, M. B. Sporn and M. E. Bolander, *J. Cell Biol.*, 1990, **110**, 2195–2207.

251 L. Bian, D. Y. Zhai, E. Tous, R. Rai, R. L. Mauck and J. A. Burdick, *Biomaterials*, 2011, **32**, 6425–6434.

252 X. Cui, K. Breitenkamp, M. G. Finn, M. Lotz and D. D. D'Lima, *Tissue Eng., Part A*, 2012, **18**, 1304–1312.

253 J. Kundu, J.-H. Shim, J. Jang, S.-W. Kim and D.-W. Cho, *J. Tissue Eng. Regener. Med.*, 2015, **9**(11), 1286–1297.

254 B. S. Yoon and K. M. Lyons, *J. Cell. Biochem.*, 2004, **93**(1), 93–103.

255 F. E. Freeman, P. Pitacco, L. H. A. Van Dommelen, J. Nulty, D. C. Browne, J.-Y. Shin, E. Alsberg and D. J. Kelly, *Sci. Adv.*, 2020, **6**(33).

256 Y. Zhu, M. Yuan, H. Y. Meng, A. Y. Wang, Q. Y. Guo, Y. Wang and J. Peng, *Osteoarthritis Cartilage*, 2013, **21**(11), 1627–1637.

257 E. Kon, R. Buda, G. Filardo, A. Di Martino, A. Timoncini, A. Cenacchi, P. M. Fornasari, S. Giannini and M. Marcacci, *Knee Surg. Sports Traumatol. Arthrosc.*, 2010, **18**, 472–479.

258 G. Filardo, E. Kon, R. Buda, A. Timoncini, A. Di Martino, A. Cenacchi, P. M. Fornasari, S. Giannini and M. Marcacci, *Knee Surg. Sports Traumatol. Arthrosc.*, 2011, **19**, 528–535.

259 E. Kon, B. Mandelbaum, R. Buda, G. Filardo, M. Delcogliano, A. Timoncini, P. M. Fornasari, S. Giannini and M. Marcacci, *Arthroscopy*, 2011, **27**, 1490–1501.

260 G. Irmak and M. Gümüşderelioğlu, *Biomed. Mater.*, 2020, **15**, 6.

261 Z. Li, X. Zhang, T. Yuan, Y. Zhang, C. Luo, J. Zhang, Y. Liu and W. Fan, *Tissue Eng., Part A*, 2020, **26**, 15–16.

262 G. Irmak and M. Gümüşderelioğlu, *Mater. Sci. Eng., C*, 2021, **125**, 112092.

263 R. Burdis and D. J. Kelly, *Acta Biomater.*, 2021, **126**, 1–14.

264 I. Martin, J. Malda and N. C. Rivron, *Curr. Opin. Organ Transplant.*, 2019, **24**, 562–567.

265 B. S. Schon, G. J. Hooper and T. B. F. Woodfield, *Ann. Biomed. Eng.*, 2017, **45**, 100–114.

266 H. Zhang, H. Huang, G. Hao, Y. Zhang, H. Ding, Z. Fan and L. Sun, *Adv. Funct. Mater.*, 2021, **31**(1), 2006697.

267 Y. Sun, Q. Wu, Y. Zhang, K. Dai and Y. Wei, *Nanomedicine*, 2021, **37**, 102426.

268 Y. Cao, P. Cheng, S. Sang, C. Xiang, Y. An, X. Wei, Z. Shen, Y. Zhang and P. Li, *Regener. Biomater.*, 2021, **8**, 3.

269 A. Dimaraki, P. J. Díaz-Payno, M. Minneboo, M. Nouri-Goushki, M. Hosseini, N. Kops, R. Narcisi, M. J. Mirzaali,



G. J. V. M. van Osch, L. E. Fratila-Apachitei and A. A. Zadpoor, *Appl. Sci.*, 2021, **11**, 7821.

270 Z. Yang, T. Zhao, C. Gao, F. Cao, H. Li, Z. Liao, L. Fu, P. Li, W. Chen, Z. Sun, S. Jiang, Z. Tian, G. Tian, K. Zha, T. Pan, X. Li, X. Sui, Z. Yuan, S. Liu and Q. Guo, *ACS Appl. Mater. Interfaces*, 2021, **13**, 23369–23383.

271 C. Di Bella, S. Duchi, C. D. O'Connell, R. Blanchard, C. Augustine, Z. Yue, F. Thompson, C. Richards, S. Beirne, C. Onofrillo, S. H. Bauquier, S. D. Ryan, P. Pivonka, G. G. Wallace and P. F. Choong, *Tissue Eng. Regener. Med.*, 2018, **12**, 611–621.

272 A. G. González Vázquez, L. A. Blokpoel Ferreras, K. E. Bennett, S. M. Casey, P. A. J. Brama and F. J. O'Brien, *Adv. Healthcare Mater.*, 2021, **10**(20), e2100878.

273 M. Chen, Y. Li, S. Liu, Z. Feng, H. Wang, D. Yang, W. Guo, Z. Yuan, S. Gao, Y. Zhang, K. Zha, B. Huang, F. Wei, X. Sang, Q. Tian, X. Yang, X. Sui, Y. Zhou, Y. Zheng and Q. Guo, *Bioact. Mater.*, 2021, **6**, 1932–1944.

274 S. E. Critchley, E. J. Sheehy, G. M. Cunniffe, P. Diaz-Payne, S. F. Carroll, O. Jeon, E. Alsberg, P. A. J. Brama and D. J. Kelly, *Acta Biomater.*, 2020, **113**, 130–143.

275 F. Berthiaume, T. J. Maguire and M. L. Yarmush, *Annu. Rev. Chem. Biomol. Eng.*, 2011, **2**, 403–430.

276 D. C. Kelly, R. M. Raftery, C. M. Curtin, C. M. O'Driscoll and F. J. O'Brien, *J. Orthop. Res.*, 2019, **37**, 1671–1680.

277 C.-C. Ma, Z.-L. Wang, T. Xu, Z.-Y. He and Y.-Q. Wei, *Biotechnol. Adv.*, 2020, **40**, 107502.

278 L. R. Baden, H. M. El Sahly, B. Essink, K. Kotloff, S. Frey, R. Novak, D. Diemert, S. A. Spector, N. Roush, C. B. Creech, J. McGettigan, S. Khetan, N. Segall, J. Solis, A. Brosz, C. Fierro, H. Schwartz, K. Neuzil, L. Corey, P. Gilbert, H. Janes, D. Follmann, M. Marovich, J. Mascola, L. Polakowski, J. Ledgerwood, B. S. Graham, H. Bennett, R. Pajon, C. Knightly, B. Leav, W. Deng, H. Zhou, S. Han, M. Ivarsson, J. Miller and T. Zaks, *N. Engl. J. Med.*, 2021, **384**, 403–416.

279 F. P. Polack, S. J. Thomas, N. Kitchin, J. Absalon, A. Gurtman, S. Lockhart, J. L. Perez, G. Pérez Marc, E. D. Moreira, C. Zerbini, R. Bailey, K. A. Swanson, S. Roychoudhury, K. Koury, P. Li, W. V. Kalina, D. Cooper, R. W. Frenck Jr., L. L. Hammitt, Ö. Türeci, H. Nell, A. Schaefer, S. Ünal, D. B. Tresnan, S. Mather, P. R. Dormitzer, U. Şahin, K. U. Jansen and W. C. Gruber, *N. Engl. J. Med.*, 2020, **383**, 2603–2615.

280 L. Schoenmaker, D. Witzigmann, J. A. Kulkarni, R. Verbeke, G. Kersten, W. Jiskoot and D. J. A. Crommelin, *Int. J. Pharm.*, 2021, **601**, 120586.

281 T. Gonzalez-Fernandez, D. J. Kelly and F. J. O'Brien, *Adv. Ther.*, 2018, **1**(7), 1800038.

282 C. E. Dunbar, K. A. High, J. K. Joung, D. B. Kohn, K. Ozawa and M. Sadelain, *Science*, 2018, **359**(6372), eaan4672.

283 X. Guo and L. Huang, *Acc. Chem. Res.*, 2012, **45**, 971–979.

284 L. S. Costard, D. C. Kelly, R. N. Power, C. Hobbs, S. Jaskaniec, V. Nicolosi, B. L. Cavanagh, C. M. Curtin and F. J. O'Brien, *Pharmaceutics*, 2020, **12**, 1219.

285 F. Cardarelli, L. D'Giacomo, C. Marchini, A. Amici, F. Salomone, G. Fiume, A. Rossetta, E. Gratton, D. Pozzi and G. Caracciolo, *Sci. Rep.*, 2016, **6**, 25879.

286 E. G. Tierney, G. P. Duffy, A. J. Hibbitts, S.-A. Cryan and F. J. O'Brien, *J. Controlled Release*, 2012, **158**, 304–311.

287 H. O. McCarthy, J. McCaffrey, C. M. McCrudden, A. Zholobenko, A. A. Ali, J. W. McBride, A. S. Massey, S. Pentlavalli, K.-H. Chen, G. Cole, S. P. Loughran, N. J. Dunne, R. F. Donnelly, V. L. Kett and T. Robson, *J. Controlled Release*, 2014, **189**, 141–149.

288 J. E. Dixon, G. Osman, G. E. Morris, H. Markides, M. Rotherham, Z. Bayoussef, A. J. El Haj, C. Denning and K. M. Shakesheff, *Proc. Natl. Acad. Sci. U. S. A.*, 2016, **113**, E291–E299.

289 D. P. Walsh, R. M. Raftery, R. Murphy, G. Chen, A. Heise, F. J. O'Brien and S.-A. Cryan, *Biomater. Sci.*, 2021, **9**, 4984–4999.

290 A. L. Laiva, R. M. Raftery, M. B. Keogh and F. J. O'Brien, *Int. J. Pharm.*, 2018, **544**(2), 372–379.

291 A. L. Laiva, F. J. O'Brien and M. B. Keogh, *Biotechnol. Bioeng.*, 2021, **118**(2), 725–736.

292 M. Suku, A. L. Laiva, F. J. O'Brien and M. B. Keogh, *J. Pers. Med.*, 2021, **11**, 4.

293 W. A. Lackington, R. M. Raftery and F. J. O'Brien, *Acta Biomater.*, 2018, **75**, 115–128.

